We are IntechOpen, the world's leading publisher of Open Access books Built by scientists, for scientists

4,800
Open access books available

122,000
International authors and editors

135M
Downloads

Our authors are among the

154
Countries delivered to

TOP 1%
most cited scientists

12.2%
Contributors from top 500 universities

CLARIVATE ANALYTICS BOOK CITATION INDEX INDEXED

WEB OF SCIENCE™

Selection of our books indexed in the Book Citation Index in Web of Science™ Core Collection (BKCI)

Interested in publishing with us?
Contact book.department@intechopen.com

Numbers displayed above are based on latest data collected.
For more information visit www.intechopen.com

10

Sensor and Actuator/Surface Failure Detection Based on the Spectral Norm of an Innovation Matrix

Chingiz Hajiyev
Istanbul Technical University
Turkey

1. Introduction

The problem of changes detection in dynamical properties of signals and systems appears in many problems of signal processing, navigation and control (Basseville & Benveniste, 1986; Benveniste *et al.*, 1987; Gadzhiev, 1992; Chen & Patton, 1999; Chan *et al.*, 1999; Hajiyev & Caliskan, 2003; Vaswani, 2004; Tykierko, 2008; Li & Jaimoukha, 2009). Abnormal measurements, sudden shifts appearing in the measuring channel, faultiness of measuring devices, changes in statistical characteristics of noises of an object or of measurements, malfunctions in the computer, and also a sharp change in the trajectory of a monitoring process, etc. should be enumerated among these changes. In real situations of exploiting an object, the problem occurs of operative detection of such changes in order to subsequently correct estimators or to make timely decisions on the necessity and character of control actions with respect to the process of technical exploitation of the object. Under this process, different methods of control and diagnostics are used.

Many fault detection methods have been developed to detect and identify sensor and actuator faults by using analytical redundancy (Zhang & Li, 1997; Rago *et al.,* 1998; Maybeck, 1999; Larson *et al.,* 2002; Lee & Lyou, 2002). In (Larson *et al.,* 2002) an analytical redundancy-based approach for detecting and isolating sensor, actuator, and component (i.e., plant) faults in complex dynamical systems, such as aircraft and spacecraft is developed. The method is based on the use of constrained Kalman filters, which are able to detect and isolate such faults by exploiting functional relationships that exist among various subsets of available actuator input and sensor output data.

A statistical change detection technique based on a modification of the standard generalized likelihood ratio (GLR) statistic is used to detect faults in real time. The GLR test requires the statistical characteristics of the system to be known before and after the fault occurs. As this information is usually not available after the fault, the method has limited applications in practice. An integrated robust fault detection and isolation (FDI) and fault tolerant control (FTC) scheme for a fault in actuators or sensors of linear stochastic systems subjected to unknown inputs (disturbances) is presented in (Lee & Lyou, 2002). The FDI modules is constructed using banks of robust two-stage Kalman filters, which simultaneously estimate the state and the fault bias, and generate residual

sets decoupled from unknown disturbances. All elements of residual sets are evaluated by using a hypothesis statistical test, and the fault is declared according to the prepared decision logic. In this work it is assumed that single fault occurs at a time and the fault treated is of random bias type. The diagnostic method presented in the article is valid only for the control surface FDI.

In (Zhang & Li, 1997; Rago *et al.,* 1998) the algorithms for detection and diagnosis of multiple failures in a dynamic system are described. They are based on the Interacting Multiple-Model (IMM) estimation algorithm, which is one of the most cost-effective adaptive estimation techniques for systems involving structural as well as parametric changes. The proposed algorithms provide an integrated framework for fault detection, diagnosis, and state estimation. In (Maybeck, 1999) Multiple model adaptive estimation (MMAE) methods have been incorporated into the design of a flight control system for the variable in-flight stability test aircraft (VISTA) F-16, providing it with the capability to detect and compensate for sensor/actuator failures. The algorithm consists of a "front end" estimator for the control system, composed of a bank of parallel Kalman filters, each matched to a specific hypothesis about the failure status of the system (fully functional or a failure in any one sensor or actuator), and a means of blending the filter outputs through a probability-weighted average. In methods described in (Zhang & Li, 1997; Rago *et al.*, 1998; Maybeck, 1999), the faults are assumed to be known, and the Kalman filters are designed for the known sensor/actuator faults. As the approach requires several parallel Kalman filters, and the faults should be known, it can be used in limited applications.

In the references (Napolitano *et al.*, 1993; Raza, *et al.*, 1994; Napolitano, *et al.*, 1996; Borairi & Wang, 1998; Alessandri, 2003) the neural network based methods to detect sensor/actuator failures are developed and discussed. In the reference (Napolitano *et al.*, 1993) a neural network is proposed as an approach to the task of failure detection following damage to an aerodynamic surface of an aircraft flight control system. This structure, used for state estimation purpose, can be designed and trained on line in flight and generates a residual signal indicating the damage as soon as it occurs. In (Raza *et al.*, 1994) the problem of detecting control surface failures of a high performance aircraft is considered. The detection model is developed using a linear dynamic model of an F/A-18 aircraft. Two parallel models detect the existence of a surface failure, whereas the isolation and magnitude of any one of the possible failure modes is estimated by a decision algorithm using either neural networks or fuzzy logic. The reference (Napolitano *et al.*, 1996) describes a study related to the testing and validation of a neural-network based approach for the problem of actuator failure detection and identification following battle damage to an aircraft control surface. Online learning neural architectures, trained with the Extended Back-Propagation algorithm, have been tested under nonlinear conditions in the presence of sensor noise. In (Borairi & Wang,1998) an approach for the fault detection and diagnosis of the actuators and sensors in non-linear systems is presented. First, a known non-linear system is considered, where an adaptive diagnostic model incorporating the estimate of the fault is constructed. Further, unknown nonlinear systems are studied and a feed forward neural network trained to estimate the system under healthy conditions. Genetic algorithms is proposed as a means of optimizing the weighting connections of neural network and to assist the diagnosis of the fault. In (Alessandri, 2003) a neural network based method to detect faults in nonlinear systems is proposed. Fault diagnosis is accomplished by means of a bank of estimators, which

provide estimates of parameters that describe actuator, plant, and sensor faults. The problem of designing such estimators for general nonlinear systems is solved by searching for optimal estimation functions. These functions are approximated by feed forward neural networks and the problem is reduced to find the optimal neural weights. The methods based on artificial neural networks and genetic algorithms do not have physical bases. Therefore according to the different data corresponding to the same event the model gives different solutions. Thus, the model should continuously be trained by using the new data.

The reference (Perhinschi *et al.*, 2002) focuses on specific issues relative to real-time on-line estimation of aircraft aerodynamic parameters at nominal and post-actuator failure flight conditions. A specific parameter identification (PID) method, based on Fourier Transform, has been applied to an approximated mathematical model of the NASA IFCS F-15 aircraft. The direct evaluation of stability and control derivatives versus the estimation of the coefficients of the state space system matrices evaluation has been considered. This method may not produce good results when the number of the stability and control derivatives is high.

In this direction of studies, it is necessary to mention the theory of diagnostics of a dynamic system by the innovation sequence of the Kalman filter (Mehra & Peschon, 1971; Willsky, 1976; Basseville & Benveniste, 1986; Gadzhiev, 1992, 1993; Hajiyev & Caliskan, 2003, 2005). The advantages of these methods are as follows: they provide the monitoring of the correctness of the result obtained by current working input actions; they do not require a priori information on the values of changes in the statistical characteristics of the innovation sequence in the case of fault; they allow one to solve the fault detection problem in real time; they require small computational expenditures for their realizations since they do not increase, in contrast to the most algorithmic methods, the dimension of the initial problem.

As is known (Mehra & Peschon, 1971), in the case where a system is normally operated, the normalized innovation sequence in the Kalman filter compatible with the model of dynamics is the white Gaussian noise with zero mean and identity covariance matrix. The faults appearing in the system of estimations lead to the changes in these statistical characteristics of the normalized innovation sequence. Therefore, in this case, the fault detection problem is reduced to the problem of fastest detection of the deviation of these characteristics from nominal.

In (Hajiyev & Caliskan, 2005) the sensor and control surface/actuator failures that affect the mean of the innovation sequence have been considered. The methods of testing the correspondence between the innovation sequence and the white noise and of revealing the change of its expectation are based on the classical statistical methods and are considered in detail in the literature (Mehra & Peschon, 1971; Hajiyev & Caliskan, 2003, 2005) therefore, it shall not be concentrated on testing these characteristics.

Testing, in real time, the covariance matrix of the innovation sequence of the Kalman filter turns out to be very complicated and not well developed, since there are difficulties in the determination of the confidence domain for a random matrix. Moreover, the existing methods of high-dimensional statistical analysis (Anderson, 1984; Kendall & Stuart, 1969) usually lead to asymptotic distributions; this sharply diminishes the operativeness of these methods. The method of testing the covariance matrix of the innovation sequence proposed in (Gadzhiev, 1992) on the basis of using the statistics of the ratio of two

quadratic forms, whose matrices are reversed sample and theoretical covariance matrices, is free from the above-mentioned shortcoming. Nevertheless, the results obtained in (Gadzhiev, 1992) are valid only in the case where the reversed matrices which enter the expression of the monitoring statistics are nonsingular.

In practice, therefore, one makes use of a scalar measure of this matrix such as the trace, sum of the matrix elements, generalized variance (determinant), eigenvalues of a matrix, etc., each characterizing one or another geometrical parameter of the correlation ellipsoid.

The algorithm for testing the trace of the covariance matrix of the innovation sequence is presented in (Mehra & Peschon, 1971). But the trace testing algorithm ignores the off-diagonal elements of the covariance matrix. Therefore this algorithm cannot detect very small changes, in the measurement channel (Hajiyev & Caliskan, 2003).

In (Gadzhiev, 1993) a confidence range has been constructed for the generalized variance of the Wishart matrix using Chebyshev inequality. However as it is known (Krinetsky *et al.*, 1979), the Chebyshev inequality gives the extended confidence range for the random variables. Therefore in this case the miss-failure probability increases.

Most of fault detection tests are based on the statistical properties of the eigenvalues of the sample covariance matrix (Bienvenu & Kopp, 1983; Wax & Kailath, 1985). In (Wu *et al.*, 1995) an algorithm based on the geometrical location of these eigenvalues has been proposed. In (Grouffaud *et al.*, 1996) a new kind of test based on an analytic expression of the ordered eigenvalues profile, obtained under noise only hypothesis. Strategy in this work consists in looking for a break in profile by comparing observed profile and noise only one. The decision is taken by comparing the error of prediction with the threshold, which is obtained by solving the integral equation. Unfortunately, the distributions entering in this equation are not analytically known, hence it is difficult to determine the threshold and perform the proposed algorithm.

There exists some interesting results on the distribution of eigenvalues, characteristic function of eigenvalues, and distribution and moments of the smallest eigenvalue of Wishart distributed matrices (Malik, 2003; Zanella *et al.*, 2008; Edelman, 1991; Everson & Stephen, 2000). But application of mentioned works to fault detection problem of multidimensional dynamic systems turns out to be very complicated since there are difficulties in determining the confidence domain (or intervals) for the eigenvalues of random matrix.

In this study, an approach to detect the aircraft sensor and actuator/surface failures based on the spectral norm of an innovation matrix is proposed. A real-time detection of sensor and actuator/surface failures affecting the mean and variance of the innovation process applied to F-16 fighter flight dynamic is examined. A decision approach to isolate the sensor and actuator/surface failures based on the Adaptive Extended Kalman Filter insensitive to sensor failures is proposed.

The structure of this chapter is as follow. In Section 2, the failure detection problem in multidimensional dynamic systems using spectral norm of the innovation matrix of the Kalman filter is formulated. The upper confidence bound of the spectral norm of a Gaussian random matrix that consists of normally distributed random variables with zero mean is found and a new failure detection approach based on the properties of the spectral norm of the innovation matrix is proposed in this Section. In Section 3 the AFTI/F-16 aircraft model description is given and the Extended Kalman filter (EKF) for the F-16 nonlinear dynamic model estimation is designed. In Section 4 an adaptive EKF

for the F-16 aircraft state estimation which is insensitive to sensor failures is designed and a decision approach to isolate the sensor and actuator/surface failure is proposed. In Section 5 some simulations are carried out for the sensor and actuator/surface failure detection problem in the AFTI/F-16 aircraft flight control system. The changes that affect the mathematical expectation and variance of the innovation sequence have been considered. Simulation results of adaptive EKF insensitive to sensor failures are given in this section too. Section 6 gives a brief summary of the obtained results and conclusions.

2. Failure Detection Using Spectral Norm of the Innovation Matrix

In diagnosing some dynamic systems, of special interest now are the methods of dynamic diagnosis that take into account influence of failures on system dynamics, in particular, revealing failures based on the analysis of the innovation sequence. Let us consider the linear dynamic system described by the equation of state

$$x(k+1) = \Phi(k+1,k)x(k) + G(k+1,k)w(k) \tag{1}$$

and the equation of measurements

$$z(k) = H(k)x(k) + V(k)\,, \tag{2}$$

where $x(k)$ is an N - dimensional vector of system state; $\Phi(k+1,k))$ is the $N \times N$ transition matrix of the system; $w(k)$ is a random N - dimensional vector of disturbances (system noise); $G(k+1,k)$ is the $N \times N$ transition matrix of system noise; $z(k)$ is the n - dimensional vector of measurements; $H(k)$ is the $n \times N$ matrix of measurements of the system; and $V(k)$ is a random n - dimensional vector of measurement noise. Assume that random vectors $w(k)$ and $V(k)$ are a Gaussian white noise. Their mean values and covariance are determined by the expressions

$$\begin{aligned} &E[w(k)] = 0; E[V(k)] = 0; \\ &E\left[w(k)w^T(j)\right] = Q(k)\delta(kj); \\ &E\left[V(k)V^T(j)\right] = R(k)\delta(kj). \end{aligned} \tag{3}$$

Here E is the operator of statistical averaging; T is the sign of transposition; and $\delta(kj)$ is the Kronecker delta symbol. Note that $\{w(k)\}$ and $\{V(k)\}$ are assumed mutually uncorrelated.

Estimate of the state vector $\hat{x}(k/k)$ and covariance matrix of estimation errors $P(k/k)$ can be found using the optimum linear discrete Kalman filter (Sage and Melsa, 1971):

$$\begin{aligned}
&\hat{x}(k/k) = \hat{x}(k/k-1) + K(k)\nu(k);\\
&\nu(k) = z(k) - H(k)\hat{x}(k/k-1);\\
&K(k) = P(k/k-1)H^{T}(k)\left[H(k)P(k/k-1)H^{T}(k) + R(k)\right]^{-1};\\
&P(k/k) = \left[I - K(k)H(k)\right]P(k/k-1);\\
&P(k/k-1) = \Phi(k,k-1)P(k-1/k-1)\Phi^{T}(k,k-1) +\\
&+ G(k,k-1)Q(k-1)G^{T}(k,k-1),
\end{aligned} \tag{4}$$

Here $K(k)$ is the gain matrix of the Kalman filter; $\nu(k)$ is the innovation sequence; I is a unit matrix; $P(k/k-1)$ is the covariance matrix of extrapolation errors and $P(k-1/k-1)$ is the covariance matrix of estimation errors at the previous step.

If there are no faults in the estimation system, then the normalized innovation sequence

$$\tilde{\nu}(k) = \left[H(k)P(k/k-1)H^{T}(k) + R(k)\right]^{-1/2}\nu(k), \tag{5}$$

in the Kalman filter (4) coordinated with the model dynamics is a Gaussian white noise with zero mean and a unit covariance matrix (Mehra and Peschon, 1971)

$$E\left[\tilde{\nu}(k)\right] = 0; E\left[\tilde{\nu}(k)\tilde{\nu}^{T}(j)\right] = P_{\tilde{\nu}} = I\delta(kj). \tag{6}$$

Failures that change system dynamics due to abrupt changes or shifts in components of the state vector, faults in computer, abnormal measurements, sudden shifts appearing in the channel of measurement, divergence of the estimation algorithm, and also such faults as a decrease in device accuracy, noise increase, etc. will result in changes of the above characteristics of the sequence of $\tilde{\nu}(k)$. Of interest is development of an on-line method of a simultaneous check of mathematical expectation and variance of the normalized innovation sequence (5) that does not require a priori information on the values of their changes in case of failure and allows one to detect on-line faults in the estimation system. To do this, two hypotheses are introduced:

γ_0 : the Kalman filter operates normally;
γ_1 : a failure takes place.

To reveal a failure, let us construct a matrix whose columns are vectors of innovation of the Kalman filter (Hajiyev, 2007). The following definitions are introduced.

Definition 1. By the innovation matrix of the Kalman filter a rectangular $n \times m$ matrix (n is the dimension of the innovation vector; $n \geq 2; m \geq 2$) is mentioned, whose columns are the innovation vectors $\nu(k)$ that correspond to m different instants of time.

Definition 2. The innovation matrix composed of the normalized innovation vectors $\tilde{\nu}(k)$ is referred as the normalized innovation matrix of the Kalman filter.

Hereinafter, to check the innovation sequence, the normalized innovation matrices A that consist of a finite number of normalized innovation vectors will be used. For a real-time check, it is expedient, at the instant of time $k(k \geq m)$, to construct the matrix $A(k)$ from a finite number m $(m \geq 2)$ of sequential innovation vectors:

$$A(k) = [\underbrace{\cdots \tilde{\nu}(k-2), \tilde{\nu}(k-1), \tilde{\nu}(k)}_{m}]. \quad (7)$$

To verify the hypothesis γ_0 and γ_1, a spectral norm of the matrix (7) below will be used.

2.1 Deriving the Upper Confidence Bound of the Spectral Norm of a Random Matrix

As is generally known (Horn and Jonson, 1986), the spectral norm $\|.\|_2$ of a real matrix $A(k)$ is determined by the formula

$$\|A(k)\|_2 \equiv \max\{(\lambda_i[A^T(k)A(k)])^{1/2}\}, \quad (8)$$

where $\lambda_i[A^T(k)A(k)]$ are eigenvalues of the matrix $A^T(k)A(k)$. Square roots of the eigenvalues of the matrix $A^T(k)A(k)$, i.e., the quantities $(\lambda_i[A^T(k)A(k)])^{1/2}$, are called the singular values of the matrix $A(k)$. Therefore, spectral norm of the matrix $A(k)$ is equal to its maximum singular value. Since the matrix $A^T(k)A(k)$ is Hermitian, $[A^T(k)A(k)]^T = A^T(k)[A^T(k)]^T = A^T(k)A(k)$, and is positive definite, i.e., for any nonzero vector $x(k)$ the relation is true

$$x^T(k)A^T(k)A(k)x(k) = (A(k)x(k), A(k)x(k)) \geq 0, \quad (9)$$

(parentheses designate here a scalar product), the singular values are real and positive. For the same reasons, computation of singular values and, consequently, also of spectral norm, is more simpler than deriving eigenvalues for an arbitrary matrix. This explains the choice of spectral norm of matrices as a controllable scalar measure in solving some diagnosis problems. Of interest is here deriving the upper bound of the spectral norm of random matrices.

In the present study, based on the calculation of a respective vector and matrix norms, an analytical expression is found for the upper bound of spectral norm of a random matrix $A(k) \in R^{n \times m}$ composed of normally distributed random variables with zero mathematical expectation. The results of the above analysis are applied to the case of dynamic diagnosis of the Kalman filter in innovation sequence.

Let the Euclidean norm (or the 2-norm) of the vector $x \in R^n$ and the spectral norm (or the 2-norm) of the matrix $A(k) \in R^{n \times m}$ be determined by the expressions

$$\begin{aligned} \|x\|_2 &= \sqrt{x_1^2 + ... + x_n^2}\,; \\ \|A\|_2 &= \sqrt{\lambda_{max}\left[A^T A\right]} = \sigma_{max}[A], \end{aligned} \tag{10}$$

where $\lambda_{max}[.]$ and $\sigma_{max}[.]$ are the maximum eigenvalue and maximum singular value of the respective matrix.

The Frobenius norm of the matrix $A = \left[a_{ij}\right] \in R^{n\times m}$ is determined as follows:

$$\|A\|_F = \sqrt{tr\left(A^T A\right)} = \sqrt{\sum_{i=1}^{n}\sum_{j=1}^{m} a_{ij}^2}, \tag{11}$$

where $tr(\cdot)$ is the trace of the matrix. The Frobenius norm and the 2-norm are related as follows (Chan *et al.*,1999):

$$\|Ax\|_2 \le \|A\|_F \|x\|_2\,, \tag{12}$$

where $A(k) \in R^{n\times m}$ and $x \in R^m$. Since $x \neq 0$, let us present expression (12) in the equivalent form

$$\frac{\|Ax\|_2}{\|x\|_2} \le \|A\|_F\,. \tag{13}$$

Inequality (13) is true for all $A(k) \in R^{n\times m}$, $x \in R^m$, $x \neq 0$, including the maximum value of the left-hand side of the inequality, i.e.,

$$\max_{x\neq 0} \frac{\|Ax\|_2}{\|x\|_2} \le \|A\|_F\,. \tag{14}$$

As is generally known (Horn and Jonson, 1986), the matrix norm associated with the respective vector norm is the relation

$$\|A\| = \max_{x\neq 0} \frac{\|Ax\|}{\|x\|}\,. \tag{15}$$

If the Euclidean norm $\|x\|_2$ is selected as the vector norm, then the respective matrix norm is the maximum singular value of the matrix *A*, i.e.,

$$\|A\| = \sigma_{max}[A]. \tag{16}$$

Regarding (14) – (16), the following inequality can be written,

$$\|A\|_2 = \sigma_{max}[A] \le \|A\|_F . \tag{17}$$

Let the matrix $A(k) \in R^{n\times m}$ be composed of normally distributed random variables with zero mathematical expectation and the mean-square deviation σ, i.e.,

$$a_{ij} \in N(0,\sigma) . \tag{18}$$

Consequently, the quantity $\sum_{i=1}^{n}\sum_{j=1}^{m} a_{ij}^2 \Big/ \sigma^2$ will have the χ^2-distribution with $k = nm - 1$ degrees of freedom (Rao, 1965). It is easy to establish a relation between $\sigma_{max}[A]$ and χ^2:

$$\sigma_{max}[A] \le \|A\|_F , \tag{19}$$

where $\|A\|_F = \sigma\sqrt{\chi^2}$.

Specifying the significance level α, the following condition can be used

$$P\left\{\chi^2 \le \chi^2_{\beta,(nm-1)}\right\} = \beta , \tag{20}$$

where $\beta = 1 - \alpha$ is the confidence probability, and tables of the χ^2-distribution to derive $\chi^2_{\beta,(nm-1)}$, which is a confidence boundary (quantile) of the χ^2-distribution with $nm - 1$ degrees of freedom. Substituting $\chi^2_{\beta,(nm-1)}$ into (19), it is obtained finally

$$\sigma_{max}[A] \le \sigma\sqrt{\chi^2_{\beta,(nm-1)}} . \tag{21}$$

Formula (21) determines the upper confidence bound for spectral norm of a random matrix *A*. Thus, an analytical expression, convenient for practical calculations, is found for the upper bound of spectral norm of a random matrix, composed from normally distributed random variables with zero mathematical expectation. The obtained result may be used in applied statistical problems, in particular, to check statistical compatibility of data of statistical simulation with the results of field tests, and in health monitoring and diagnosis of multidimensional technical systems.

2.2 Failure Detection Using Spectral Norm of the Innovation Matrix

Since the random normalized innovation matrix (7) consists of normally distributed stochastic elements with zero mathematical expectation and a finite variance $a_{ij} \in N(0,1)$, inequality (21) may be used for solution of the above diagnosis problem. Expression (21) characterizes the relation between the mean-square value σ of the elements of a random matrix A and its spectral norm and may be used to derive the upper confidence boundary of the spectral norm of matrix (7). In this case, one may state that if elements a_{ij} of the controlled normalized innovation matrix of the Kalman filter obey the distribution $N(0,1)$, then inequality (21) should be fulfilled. Non-fulfillment of inequality (21) points to the shift of zero mean of the elements a_{ij}, a change of the unit variance or to difference of $\{a_{ij}\}$ from white noise. If the case $\sigma = 1$ is considered, then inequality (21) can be written in a more simple form:

$$\sigma_{max}[A] \le \sqrt{\chi^2_{\beta,(nm-1)}} \ . \tag{22}$$

As is seen from expression (22), in the case being considered, the upper confidence boundary of the spectral norm of the normalized innovation matrix of the Kalman filter is determined by the dimension of the innovation vector (or dimension of the measurement vector), the number of sequential innovation vectors used, and the confidence probability selected.

In view of that stated above, in solving the diagnosis problem posed, the decision rule concerning the hypotheses introduced has the form

$$\gamma_0 : \sigma_{max}[A] \le \sqrt{\chi^2_{\beta,(nm-1)}} \ , \ \forall k \ge m;$$
$$\gamma_1 : \exists k \ge m, \sigma_{max}[A] > \sqrt{\chi^2_{\beta,(nm-1)}} \ . \tag{23}$$

The boundary for the spectral norm of the normalized innovation matrix found is quite simple and allows one to check on-line simultaneously mathematical expectation and variance of the innovation sequence. Under operating conditions, the algorithm proposed can be reduced to the following sequence of calculations performed at each step of measurements.

1. Using expressions (4), calculate the Kalman estimate for the vector of system state and the value of the vector of the normalized innovation sequence at the current step k.

2. Compose the normalized innovation matrix for the Kalman filter according to (7) for the given $n \ge 2, m \ge 2$ and $k \ge m$.

3. Determine eigenvalues of the matrix $A^T(k)A(k)$ as solutions of the equation $\det(A - \lambda I) = 0$ and the spectral norm

$$\|A(k)\|_2 = \sigma_{max}[A(k)] = \max\left\{\left(\lambda_i\left[A^T(k)A(k)\right]\right)^{1/2}\right\}. \tag{24}$$

4. Check realization of inequality (22) and make decision on detection of a failure in the Kalman filter based on the decision rule (23).

5. Repeat the sequence of calculations, beginning with step 1, for the next instant of time $k+1$.

Qualitative characteristics of the proposed algorithm of failure revealing are probabilities of a correct detection and a false alarm. These characteristics are calculated in a usual way with the use of the table of the χ^2-distribution (Grishin and Kazarinov, 1985). Deriving the required characteristics involves a large volume of mathematical simulation for a justified choice of m number of innovation vectors $\nu(k)$, that correspond to m different instants of time, from which the matrix of innovation A is composed. A too large m smoothes effects caused by the system failure, and a too small m, increases probability of a false alarm.

3. Design of the EKF for the F-16 Aircraft State Estimation

3.1 F-16 Aircraft Model Description

The technique for failure detection is applied to an unstable multi-input multi-output model of an AFTI/F-16 fighter. The fighter is stabilized by means of a linear quadratic optimal controller. The control gain brings all the eigenvalues that are outside the unit circle, inside the unit circle. It also keeps the mechanical limits on the deflections of control surfaces. The model of the fighter is as follows (Lyshevski, 1997):

$$x(k+1) = Ax(k) + Bu(k) + F(x(k)) + Gw(k) \tag{25}$$

where $x(k)$ is the 9-dimensional state vector of the aircraft, A is the transition matrix of order 9x9 of the aircraft, B is the control distribution matrix of order 9x6 of the aircraft, $u(k)$ is the 6-dimensional control input vector, $F(x(k))$ is the 9-dimensional vector of nonlinear elements of system, $w(k)$ is the random 9-dimensional vector of system noises with zero mean and the covariance matrix $E\left[w(k)w^T(j)\right] = Q(k)\delta(kj)$, G is the transition matrix of the system noises.

The aircraft state variables are:

$$x = \left[v, \alpha, q, \theta, \beta, p, r, \phi, \psi\right]^T,$$

where, v is the forward velocity, α is the angle of attack, q is the pitch rate, θ is the pitch angle, β is the side-slip angle, p is the roll rate, r is the yaw rate, ϕ is the roll angle, and ψ is the yaw angle.

The fighter has six control surfaces and hence six control inputs are:

$$u = \left[\delta_{HR}, \delta_{HL}, \delta_{FR}, \delta_{FL}, \delta_C, \delta_R\right],$$

where δ_{HR} and δ_{HL} are the deflections of the right and left horizontal stabilizers, δ_{FR} and δ_{FL} are the deflections of the right and left flaps, δ_C and δ_R are the canard and rudder deflections. The following hard bounds (mechanical limits) on the deflections of control surfaces are assumed: $|\delta_{HR}, \delta_{HL}| \le 0.44$ rad, $|\delta_{FR}, \delta_{FL}| \le 0.35$ rad, $|\delta_C| \le 0.47$ rad and $|\delta_R| \le 0.52$ rad. A, B and F(x) for the sampling period of 0.03 s. are:

$$A=\begin{bmatrix} 0.9995 & 0.2457 & -0.0273 & -0.2885 & -0.0391 & -0.0075 & -0.002 & 0 & 0 \\ -0.0001 & 0.9663 & 0.0291 & 0 & 0.0011 & 0.0017 & 0.0003 & 0 & 0 \\ 0 & 0.1135 & 0.9765 & 0 & 0.0007 & 0.0002 & 0.0012 & 0 & 0 \\ 0 & 0.0017 & 0.0296 & 1 & 0 & 0 & 0 & 0 & 0 \\ -0.0001 & 0.0048 & 0.0011 & 0.0288 & 0.977 & 0.0037 & -0.0268 & 0 & 0 \\ 0.0001 & 0.0165 & 0.0005 & -0.0198 & -1.3515 & 0.8977 & 0.025 & 0 & 0 \\ 0 & -0.0268 & 0.0015 & 0.0041 & 0.2716 & -0.0003 & 0.9811 & 0 & 0 \\ 0 & 0.0003 & 0 & -0.0002 & -0.0207 & 0.0285 & 0.0003 & 1 & 0 \\ 0 & -0.0004 & 0 & 0 & 0.0041 & 0 & 0.0297 & 0 & 1 \end{bmatrix}$$

$$B=\begin{bmatrix} 0.071 & 0.0067 & -0.011 & -0.0117 & -0.0004 & -0.0001 \\ -0.009 & -0.0088 & -0.0091 & -0.009 & 0 & 0 \\ -0.2818 & -0.2819 & -0.0746 & -0.0746 & 0 & 0 \\ -0.0042 & -0.0042 & -0.0011 & -0.0011 & 0 & 0 \\ -0.001 & 0.0007 & -0.0006 & 0.0005 & 0.0123 & 0.0018 \\ -0.0822 & 0.0819 & -0.0881 & 0.0879 & 0.0122 & 0.025 \\ 0.0921 & -0.0924 & 0.0233 & -0.0232 & 0.02 & -0.0132 \\ -0.0013 & 0.013 & -0.013 & 0.013 & 0.0002 & 0.0004 \\ 0.0014 & -0.0014 & 0.0003 & -0.0003 & 0.0003 & -0.0002 \end{bmatrix}$$

$$F(x)=\begin{bmatrix} F_v \\ F_\alpha \\ F_q \\ F_\theta \\ F_\beta \\ F_p \\ F_r \\ F_\phi \\ F_\psi \end{bmatrix} = \begin{bmatrix} 0 \\ -0.03pc\alpha \tan\beta - 0.03rs\alpha \tan\beta \\ 0.028pr - 0.00018p^2 + 0.00018r^2 \\ 0.03q\cos\phi - 0.03r\sin\phi \\ 0.03p\sin\alpha - 0.03r\cos\alpha \\ 0.00026qp - 0.017qr \\ -0.025qp - 0.00026qr \\ 0.03q\tan\theta\sin\phi + 0.03r\tan\theta\cos\phi \\ 0.03q\cos^{-1}\theta\sin\phi + 0.03r\cos^{-1}\theta\cos\phi \end{bmatrix}$$

Below the Extended Kalman Filter (EKF) to estimate the F-16 aircraft motion is designed.

3.2 Deriving of the EKF

Let us define the estimated vector as:

$$x^T(k) = [v(k), \alpha(k), q(k), \theta(k), \beta(k), p(k), r(k), \phi(k), \psi(k)]$$

and apply the Kalman filter to estimate this vector. The nonlinear mathematic model for the longitudinal and lateral F-16 aircraft motion is given in (25).
The measurement equations can be written as:

$$z(k) = Hx(k) + V(k), \tag{26}$$

where H is the measurement matrix, which is 9×9 unit matrix, $V(k)$ is the measurement noise and its mean and correlation matrix respectively are:

$$E[V(k)] = 0; E[V(k)V^T(j)] = R(k)\delta(kj).$$

By using quasi-linearization method let us linearize the equation (25):

$$\begin{aligned} x(k) = {} & A\hat{x}(k-1) + B\hat{u}(k-1) + F(\hat{x}(k-1)) + A[x(k-1) - \hat{x}(k-1)] + \\ & F_x(k-1)[x(k-1) - \hat{x}(k-1)] + B[u(k-1) - \hat{u}(k-1)] + Gw(k-1) \end{aligned} \tag{27}$$

where $F_x = \left[\frac{\partial F}{\partial x}\right]_{\hat{x}(k-1)}$.

Among the procedures of estimation theory, the Bayes procedure has the most accuracy because it is based on both the experimental data in likelihood function and a priori data expressed by a priori density of the estimated parameters. The more data, the more accuracy yields. Moreover, the Bayes procedure does not require the system to be linear and stationary, and produces a solution for the filtering when the initial conditions of the state vector are unknown (Gadzhiev, 1996). Therefore, the Bayes procedure to filter the state vector of the aircraft motion is preferred. A posteriori distribution density of the state vector is given by the Bayes formula:

$$P\left[x(k)/Z^k\right] = P\left[x(k)/Z^{k-1}, z(k)\right] = \frac{P\left[x(k)/Z^{k-1}\right]}{P\left[z(k)/Z^{k-1}\right]} P\left[z(k)/x(k), Z^{k-1}\right], \tag{28}$$

where $Z^k = \{z(1), z(2), z(3), \ldots, z(k)\}$; $Z^{k-1} = \{z(1), z(2), \ldots, z(k-1)\}$.
When the probability density functions in (28) are substituted and the conditional mathematical expectation of the a posteriori probability density function is taken as the optimum estimation value, the following recursive EKF algorithm for the state vector estimation of the F-16 aircraft motion is obtained as (Caliskan and Hajiyev, 2003):

Equation of the estimation value

$$\hat{x}(k) = \hat{x}(k/k-1) + K(k)v(k) \tag{29}$$

Equation of the extrapolation value

$$\hat{x}(k/k-1) = A\hat{x}(k-1) + B\hat{u}(k-1) + F(\hat{x}(k-1)) \tag{30}$$

The innovation sequence

$$v(k) = z(k) - H\left[A\hat{x}(k-1) + B\hat{u}(k-1) + F(\hat{x}(k-1))\right] \tag{31}$$

The gain matrix of filter

$$K(k) = P(k)H^{T}(k)R^{-1}(k) \tag{32}$$

The covariance matrix of estimation errors

$$P(k) = M(k) - M(k)H^{T}\left[HM(k)H^{T} + R(k)\right]^{-1}HM(k) \tag{33}$$

The covariance matrix of extrapolation errors

$$\begin{aligned} M(k) &= AP(k-1)A^{T} + BD_{u}(k-1)B^{T} \\ &+ F_{x}(k-1)P(k-1)F_{x}^{T}(k-1) + GQ(k-1)G^{T} \end{aligned} \tag{34}$$

where D_u is the covariance matrix of the control input error, $Q(k-1)$ is the covariance matrix of system noise.

4. Adaptive EKF Insensitive to Sensor Failures

An adaptive EKF for the F-16 aircraft state estimation may be designed in order to isolate the detected sensor and actuator/surface failures. The following approach for the solution of the filtration problem is proposed for this case (Hajiyev, 2006). In the case of normal operation of measurement system, the filter works according to the conventional EKF algorithm (29)-(34). But if the condition of the operation of the measurement system does not correspond to the models, used in the synthesis of the filter, then the gain coefficient (32) of the discrepancy automatically changes due to the change in the covariance matrix of the innovation sequence according to the rule

$$P_{v}(k) = HM(k)H^{T} + S(k)R(k) \tag{35}$$

in which weight coefficient $S(k)$ is calculated from the discrepancy (31) analysis results. In this case the filter gain coefficient (32) can be written in the form of

$$K(k) = M(k)H^T\left[HM(k)H^T + S(k)R(k)\right]^{-1} \tag{36}$$

According to the proposed approach the gain coefficient (32) is changed when the following condition is valid

$$\begin{aligned} &tr\{v(k)v^T(k)\} \geqslant tr\{E[v(k)v^T(k)]\} = \\ &tr\{E[H(x(k) - \hat{x}(k/k-1)) + v(k)] \times [H(x(k) - \hat{x}(k/k-1)) + v(k)]^T\} = \\ &tr\{HM(k)H^T + R(k)\} \end{aligned} \tag{37}$$

where $tr(.)$ is the trace of matrix. When a significant change in the conditions of the operation of the measurement system occurs, the prediction of observations in (31), $H\hat{x}(k/k-1)$, will considerably differ from the observation results $z(k)$. Consequently, the sum of the discrepancy squares on the left side of (37) will characterize the real filtration error, while the right side determines the theoretical accuracy of the innovation sequence, obtained on the basis of a priori information. If condition (38) is met, then the real filtration error exceeds the theoretical error. Therefore, it is necessary to correct the filter gain matrix (32). In this case by substituting (35) in (37) the following equation can be obtained;

$$tr\{v(k)v^T(k)\} = tr\{HM(k)H^T\} + S(k)tr\{R(k)\} \tag{38}$$

Hence taking the expression $tr\{v(k)v^T(k)\} = v^T(k)v(k)$ into consideration, the following formula for the weighting factor $S(k)$ is obtained:

$$S(k) = \frac{v^T(k)v(k) - tr\{HM(k)H^T\}}{tr\{R(k)\}} \tag{39}$$

Using (35), (36) and (39) in the estimation algorithm (29) -(34) gives the possibility to accomplish the adaptation of the filter to the change of measurement system operation conditions. If the left side of the expression (37) is greater than the right side, the value of coefficient $S(k)$ will increase. This corresponds to the beginning of the adaptation of filter. Consequently, both the covariance matrix of innovation sequence $P_v(k)$ (35) and the filter gain matrix $K(k)$ (32) increase, and that cause to the strengthening of the corrective influence of discrepancy in (29) which makes the estimation value $\hat{x}(k)$ approach to the actual value $x(k)$. This will lead to the decrease of discrepancy $v(k)$ and coefficient $S(k)$, weakening of the corrective influence of discrepancy, etc.
The final expressions of the proposed adaptive filtration algorithm with the filter gain correction insensitive to measurement faults can be written in the following form:

$$\hat{x}(k) = \hat{x}(k/k-1) + K(k)v(k)$$

$$\hat{x}(k/k-1) = A\hat{x}(k-1) + B\hat{u}(k-1) + F(\hat{x}(k-1))$$

$$v(k) = z(k) - H\left[A\hat{x}(k-1) + B\hat{u}(k-1) + F(\hat{x}(k-1))\right]$$

$$K(k) = P(k)H^T(k)\left[S(k)R(k)\right]^{-1}$$

$$P(k) = M(k) - M(k)H^T\left[P_v(k)\right]^{-1}HM(k) \qquad (40)$$

$$P_v(k) = HM(k)H^T + S(k)R(k)$$

$$S(k) = \frac{v^T(k)v(k) - tr\{HM(k)H^T\}}{tr\{R(k)\}}$$

$$M(k) = AP(k-1)A^T + BD_u(k-1)B^T + F_x(k-1)P(k-1)F_x^T(k-1) + GQ(k-1)G^T$$

where $P_v(k)$ is the covariance matrix of the innovation sequence, and $S(k)$ is the weighting factor. The other filter parameters in (40) are same with the ones given in the expressions (29)-(34).

In contrast to the EKF algorithm (29)-(34), in which the filter gain $K(k)$ changes by program, in the proposed algorithm the current measurements have larger weight, since the coefficients of matrix $K(k)$ are corrected by the results of each observation. This algorithm is adapted to the measurement system operation conditions by the approximation of the theoretical covariance matrix $P_v(k)$ to the real covariance matrix of the innovation sequence, due to the change in the weighting factor $S(k)$. Mentioned change is accomplished because of regarding the matrix $v(k)v^T(k)$, which characterizes the real filtration error. Proposed adaptive EKF for the F-16 aircraft state estimation will ensure the guaranteed adaptation of the filter to the change of the measurement system operation conditions, consequently it will become insensitive to sensor failures.

The designed adaptive EKF (40) is not an optimum filter, unlike the EKF (29)-(34), because of the $S(k)$ factor. Even in the absence of a failure, the estimation error could be larger than that of the conventional filtration algorithm (29)-(34). Therefore, adaptive algorithm is operated only when the measurements are faulty or in order to isolate the detected sensor and actuator/surface failures. In all other cases procedure is run optimally with regular EKF (29)-(31).

4. Simulation Results of Failure Detection and Adaptive EKF Algorithms

The technique for failure detection is applied to multi-input multi-output model of an AFTI/F-16 fighter (25). The measurements are processed using Kalman filter (29)-(32) that allows us to determine the estimate of the state vector of F-16 aircraft and the covariance matrix of the estimate errors at each k^{th} step.

If there are no faults in the estimation system, then the normalized innovation sequence

$$\tilde{\nu}(k) = \left[HM(k)H^T + R(k)\right]^{-1/2} \nu(k), \tag{41}$$

of the EKF (29)-(32) is a Gaussian white noise with zero mean and a unit covariance matrix. Sensor and control surface/actuator failures will result with changes in the above characteristics of the sequence of $\tilde{\nu}(k)$. To verify the hypothesis γ_0 and γ_1, let us use a spectral norm of the matrix constructed as (7).

In the simulations, $m = 10; n = 9; \beta = 0.997$ are taken, and the threshold value $\sqrt{\chi^2_{\beta,(nm-1)}}$ is found as 11.4. Decisions as to reveal a failure in the system are made based on the rule (23). The results of simulations are shown in Figs. 1–16.

4.1 A Sensor Failure (Shift in the Pitch Rate Gyroscope)

Shift in the pitch rate gyroscope is simulated at iteration 30 as follows;

$$z_q(k) = q(k) + V_q(k) + 3\,,\ (k \geqslant 30)\,. \tag{42}$$

The graph of the spectral norm $\sigma_{max}[A]$ is shown in Figure 1 when a shift occurs in the pitch rate gyroscope.

As seen in Figure 1, until the sensor failure occurs $\sigma_{max}[A]$ is lower than the threshold. When a failure occurs in the pitch rate gyroscope, $\sigma_{max}[A]$ grows rapidly, and after 1 iteration it exceeds the threshold. Hence γ_1 hypothesis is judged to be true. This failure causes a change in the mean of the innovation sequence. The innovation sequences in case of a shift in the pitch rate gyroscope are shown in Figures 2-4.

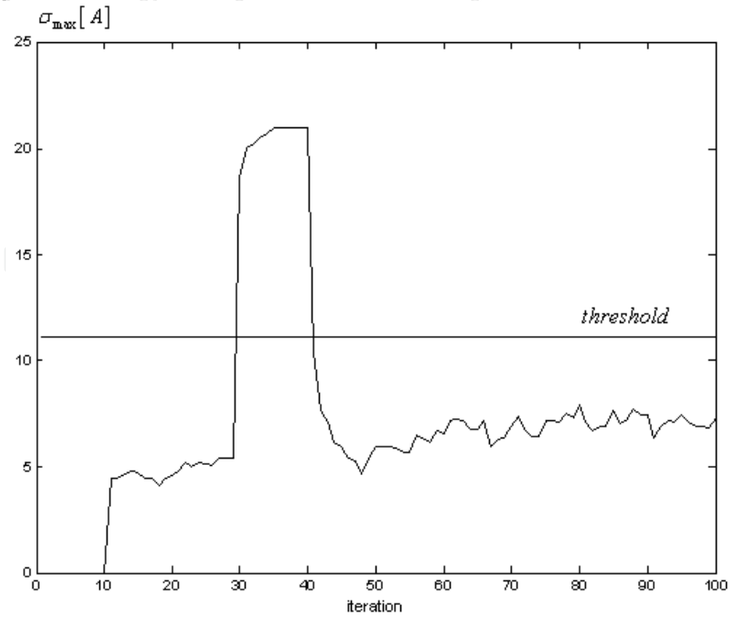

Fig. 1. Behavior of the spectral norm $\sigma_{max}[A]$ in case of a shift in the pitch rate gyroscope

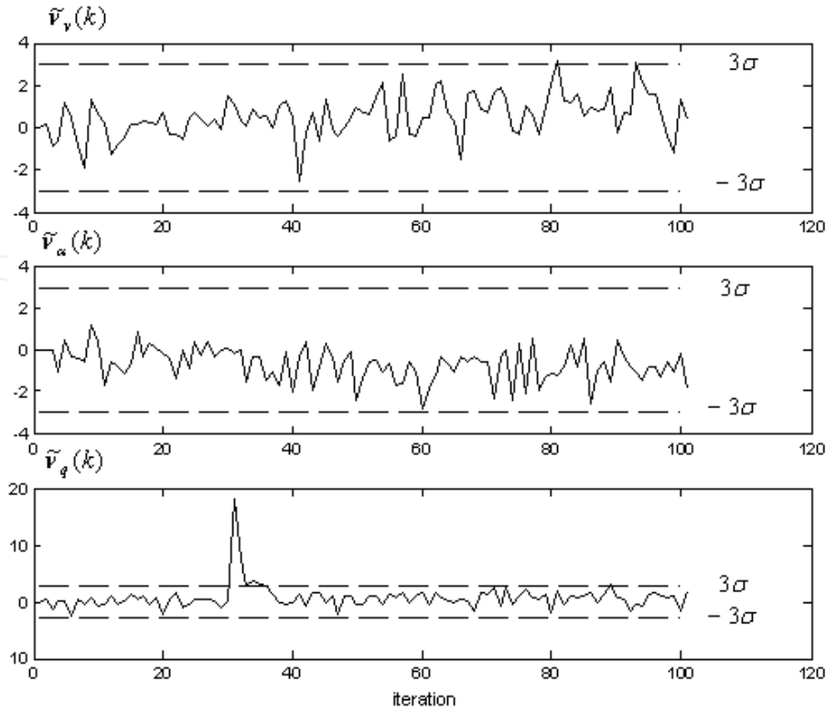

Fig. 2. Normalized Innovation Sequences $\tilde{\nu}_v(k), \tilde{\nu}_\alpha(k), \tilde{\nu}_q(k)$ in the case of a shift in the pitch rate gyroscope

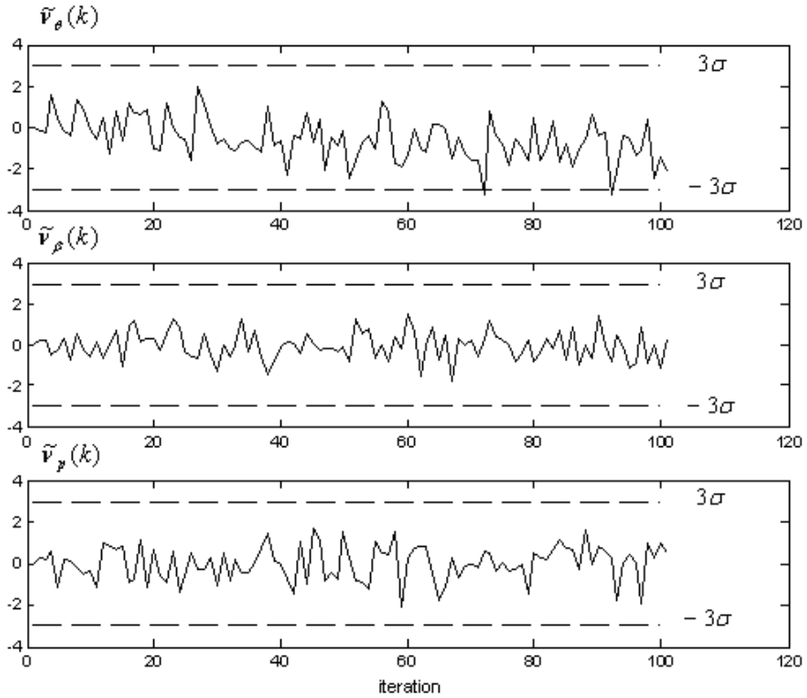

Fig. 3. Normalized Innovation Sequences $\tilde{\nu}_\theta(k)$, $\tilde{\nu}_\beta(k), \tilde{\nu}_p(k)$ in the case of a shift in the pitch rate gyroscope

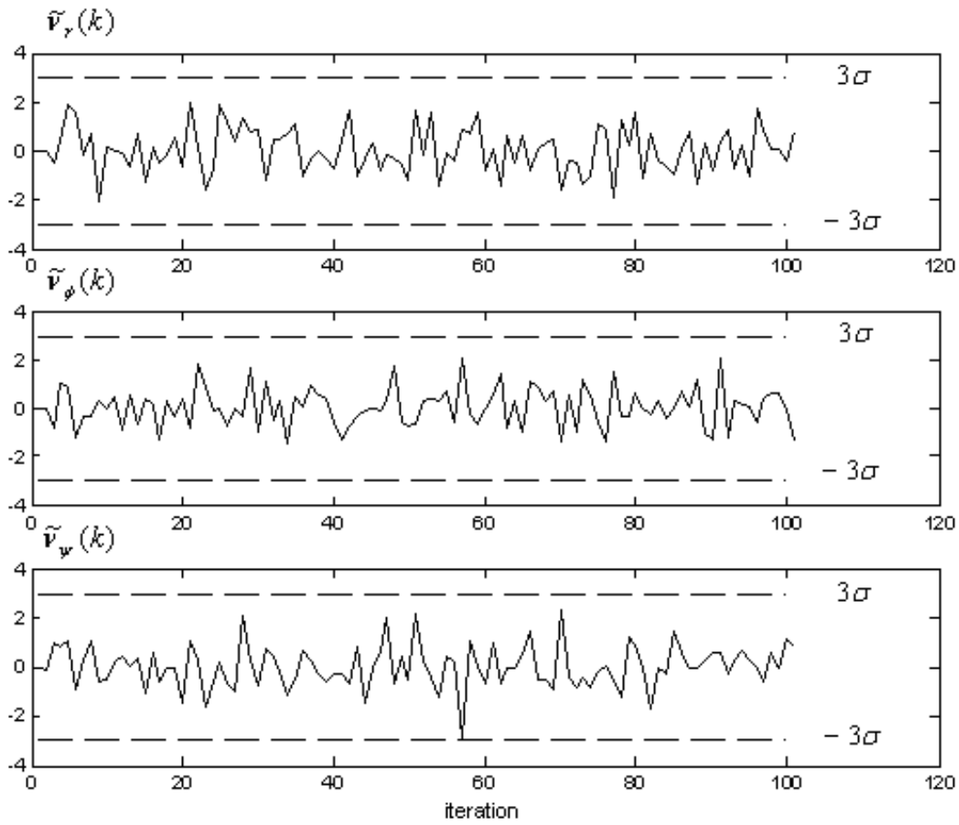

Fig. 4. Normalized Innovation Sequences $\tilde{\nu}_r(k)$, $\tilde{\nu}_\phi(k)$, $\tilde{\nu}_\psi(k)$ in the case of a shift in the pitch rate gyroscope

4.2 A Sensor Failure (the Noise Variance in the Pitch Rate Gyroscope is Changed)

The noise variance in the pitch rate gyroscope is changed at iteration 30 as follows;

$$z_q(k) = q(k) + 3V_q(k), \ (k \geqslant 30). \tag{43}$$

Figure 5 shows that the value of $\sigma_{max}[A]$ sharply increases after the 30^{th} step and intersects its admissible bound at the step $k = 42$. As a result, based on the decision rule (23), estimation system failure is noted. This failure causes a change in the variance of the innovation sequence. The innovation sequences in case of changes in the noise variance of the pitch rate gyroscope are shown in Figures 6-8.

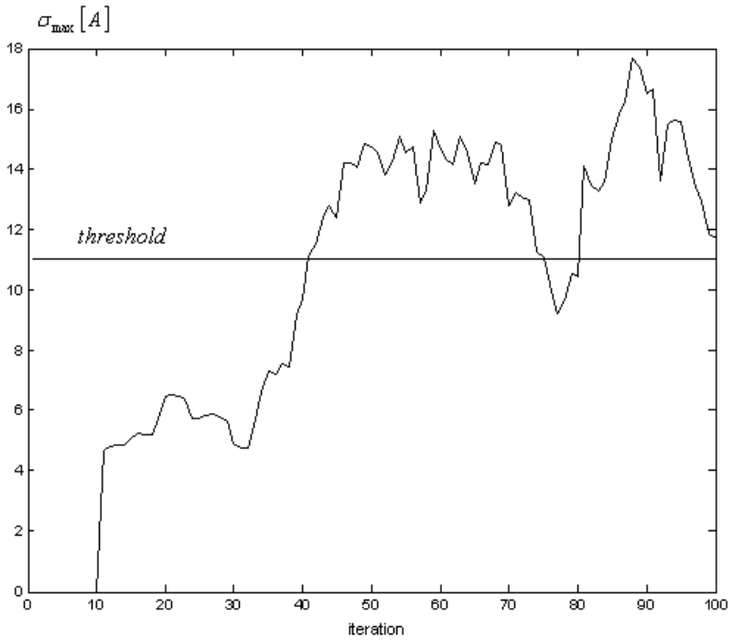

Fig. 5. Behavior of the spectral norm $\sigma_{max}[A]$ in case of changes in the noise variance of the pitch rate gyroscope

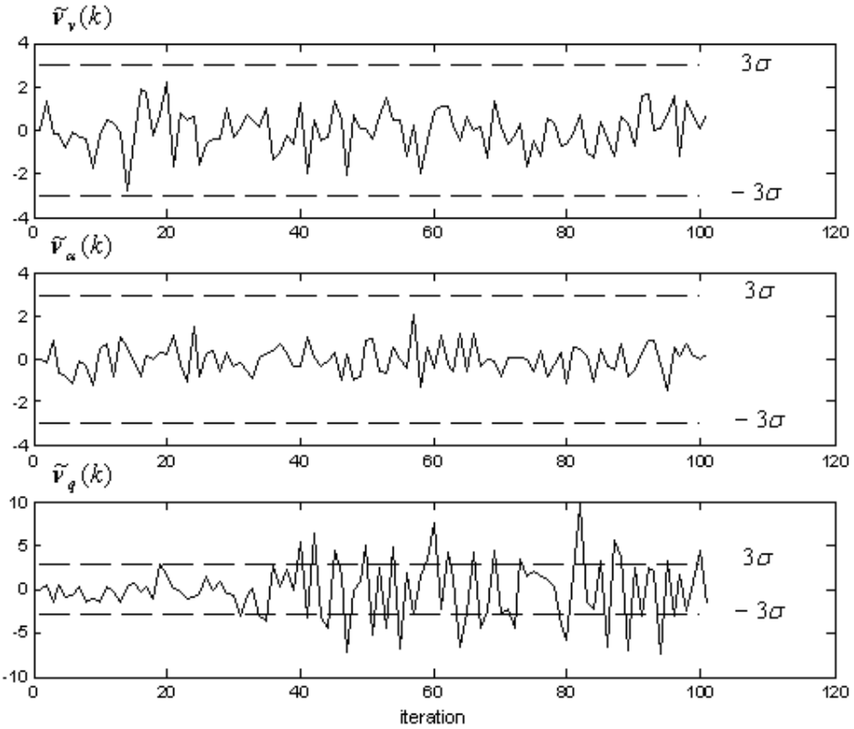

Fig. 6. Normalized Innovation Sequences $\tilde{\nu}_v(k), \tilde{\nu}_\alpha(k), \tilde{\nu}_q(k)$ in case of changes in the noise variance of the pitch rate gyroscope

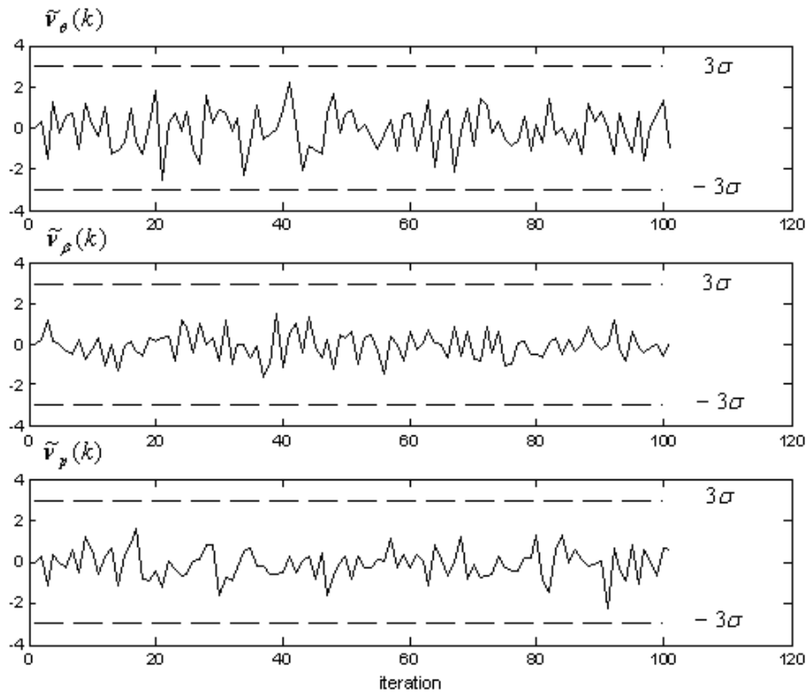

Fig. 7. Normalized Innovation Sequences $\tilde{\nu}_\theta(k)$, $\tilde{\nu}_\beta(k)$, $\tilde{\nu}_p(k)$ in case of changes in the noise variance of the pitch rate gyroscope

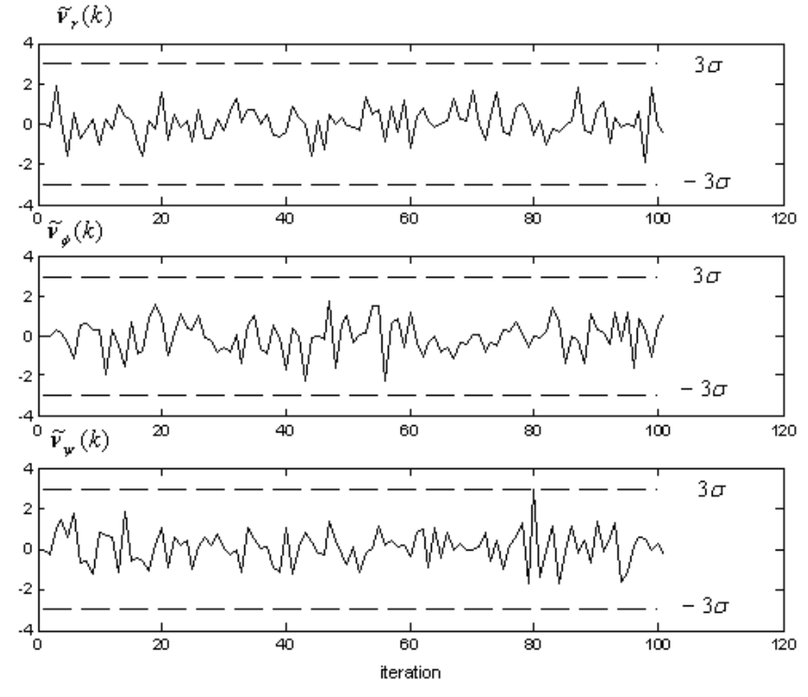

Fig. 8. Normalized Innovation Sequences $\tilde{\nu}_r(k)$, $\tilde{\nu}_\phi(k)$, $\tilde{\nu}_\psi(k)$ in case of changes in the noise variance of the pitch rate gyroscope

4.3 The Actuator Motor Failure

Two kinds of failures can occur in an actuator: actuator motor failure, and control surface failure. For simulation of the actuator motor failure, the control input δ_{HR} (deflection of the right horizontal stabilizer) has been changed to $\delta_{HR}(k) = \delta_{HR}(k) + 1^{\circ}$, $(k \geq 30)$ at iteration 30. The graph of the spectral norm $\sigma_{max}[A]$ is shown in Figure 9 when a shift occurs in the actuator motor at the step 30. This failure causes a change in the mean of the innovation sequence. As seen in Figure 9, until the actuator failure occurs, spectral norm $\sigma_{max}[A]$ is lower than the threshold. When a failure occurs in the actuator $\sigma_{max}[A]$ grows rapidly, and after 3 steps it exceeds the threshold. Hence γ_1 hypothesis is judged to be true**.** The innovation sequences in the case of actuator motor failure are shown in Figures 10-12.

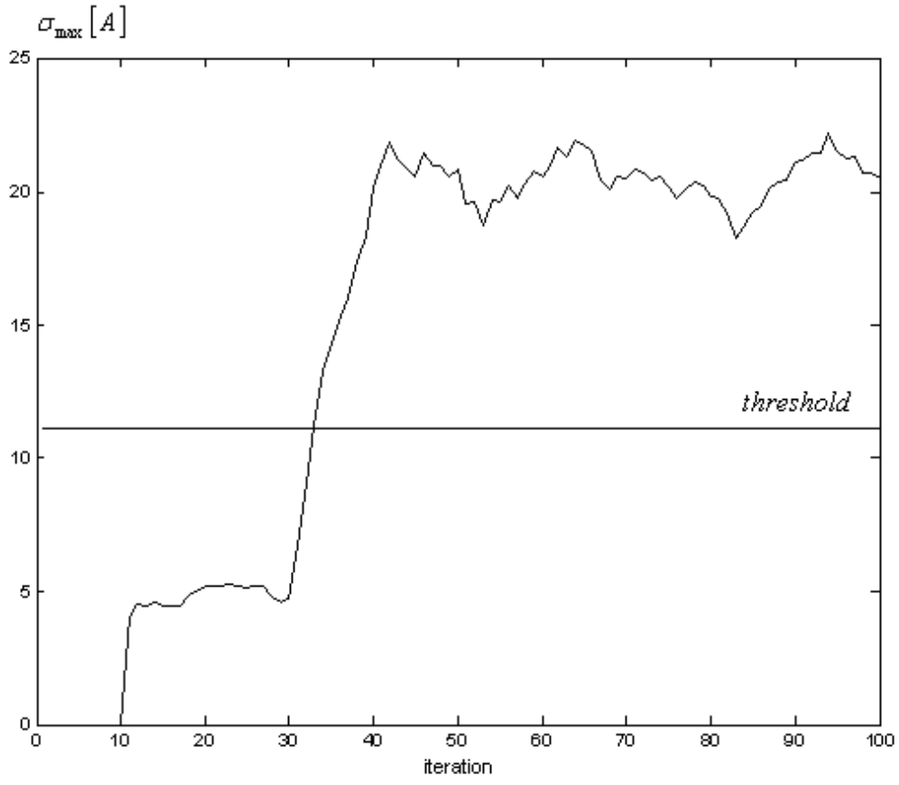

Fig. 9. Behavior of the spectral norm $\sigma_{max}[A]$ in case of actuator motor failure

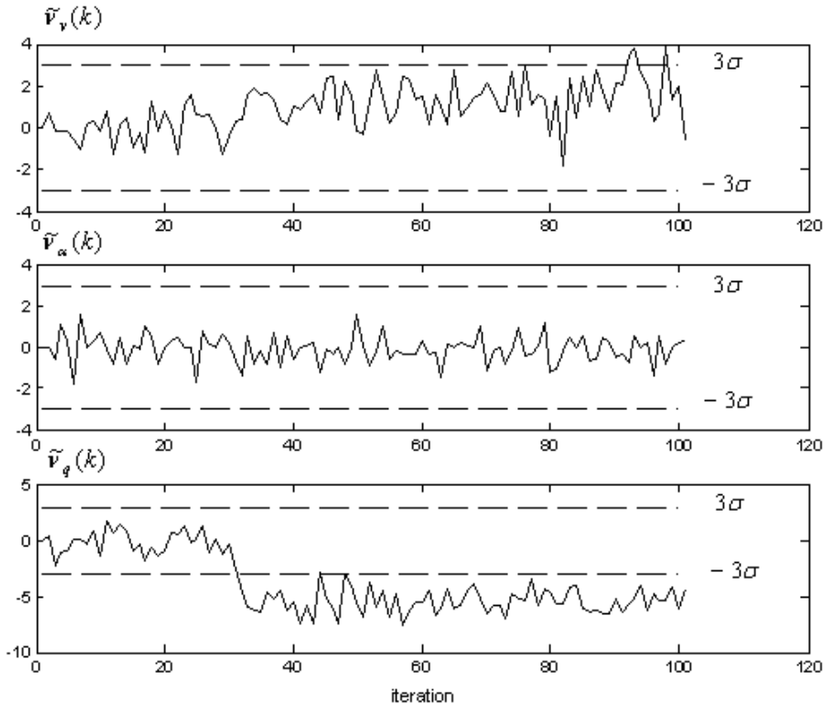

Fig. 10. Normalized Innovation Sequences $\tilde{\nu}_v(k), \tilde{\nu}_\alpha(k), \tilde{\nu}_q(k)$ in case of actuator motor failure

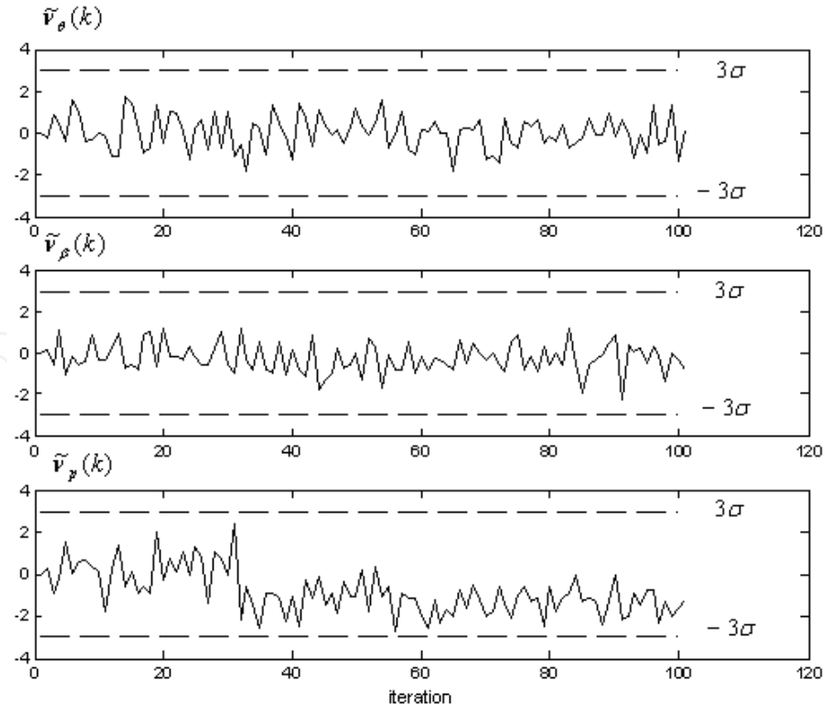

Fig. 11. Normalized Innovation Sequences $\tilde{\nu}_\theta(k)$, $\tilde{\nu}_\beta(k), \tilde{\nu}_p(k)$ in case of actuator motor failure

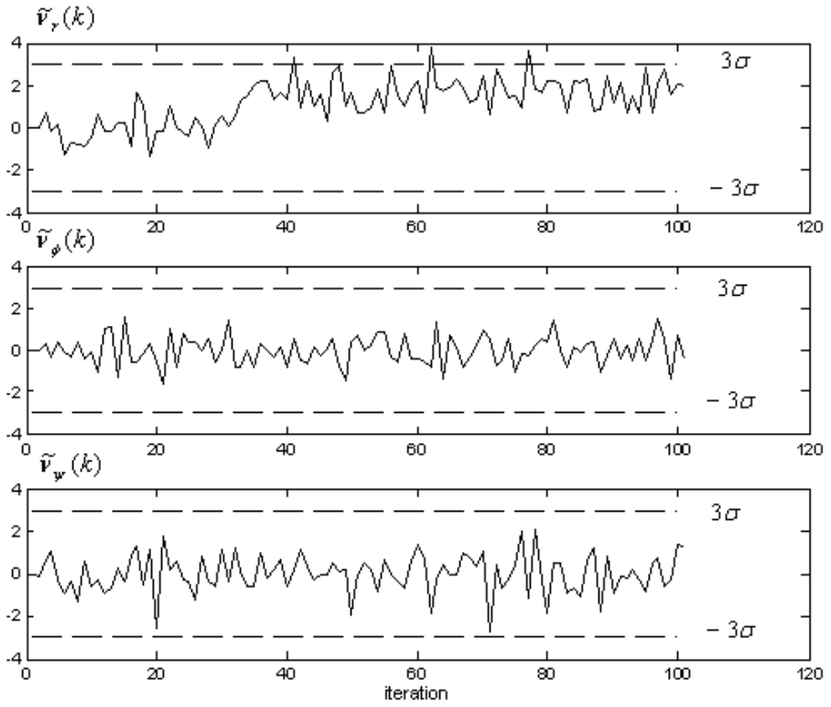

Fig. 12. Normalized Innovation Sequences $\tilde{\nu}_r(k)$, $\tilde{\nu}_\phi(k)$, $\tilde{\nu}_\psi(k)$ in case of actuator motor failure

4.4 The Control Surface Failure

The proposed failure detection algorithm is used below to detect the control surface failures. The control derivatives corresponding to the first control surface (right horizontal stabilizer) has been changed as follows at iteration 30;

$$B(i,1) = B(i,1) + 0.08;\ i = \overline{1,9},\ (k \geq 30) \tag{44}$$

The graph of the spectral norm $\sigma_{max}[A]$ is shown in Figure 13 when a shift occurs in the control surface. As seen in Figure 13, until the control surface failure occurs, $\sigma_{max}[A]$ is lower than the threshold. When a fault occurs in the control surface $\sigma_{max}[A]$ grows rapidly, and after 28 iterations it exceeds the threshold. Hence γ_1 hypothesis is judged to be true. This failure causes a change in the mean of the innovation sequence. The innovation sequences in case of control surface failure are shown in Figures 14-16.

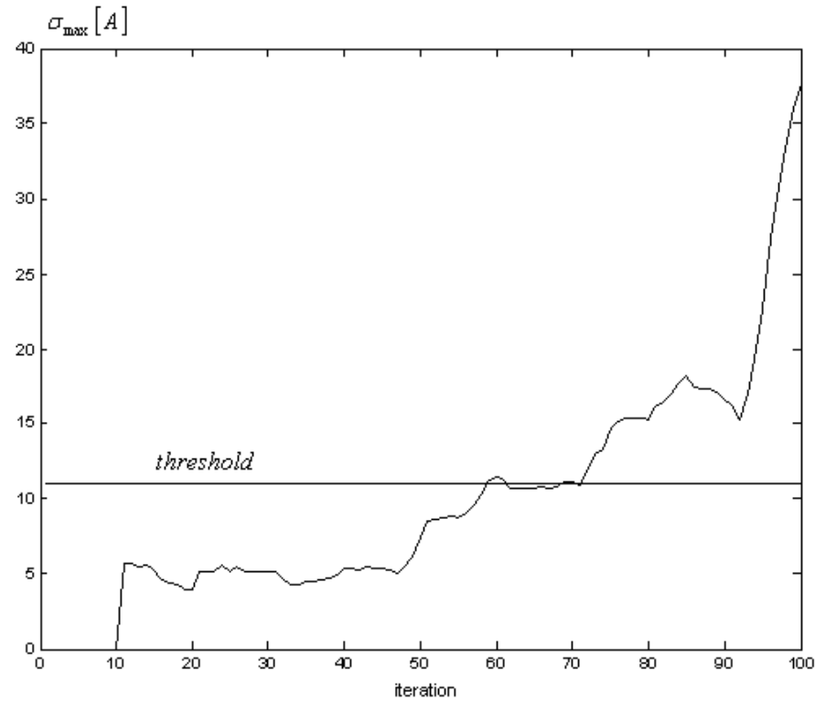

Fig. 13. Behavior of the spectral norm $\sigma_{max}[A]$ in case of control surface failure

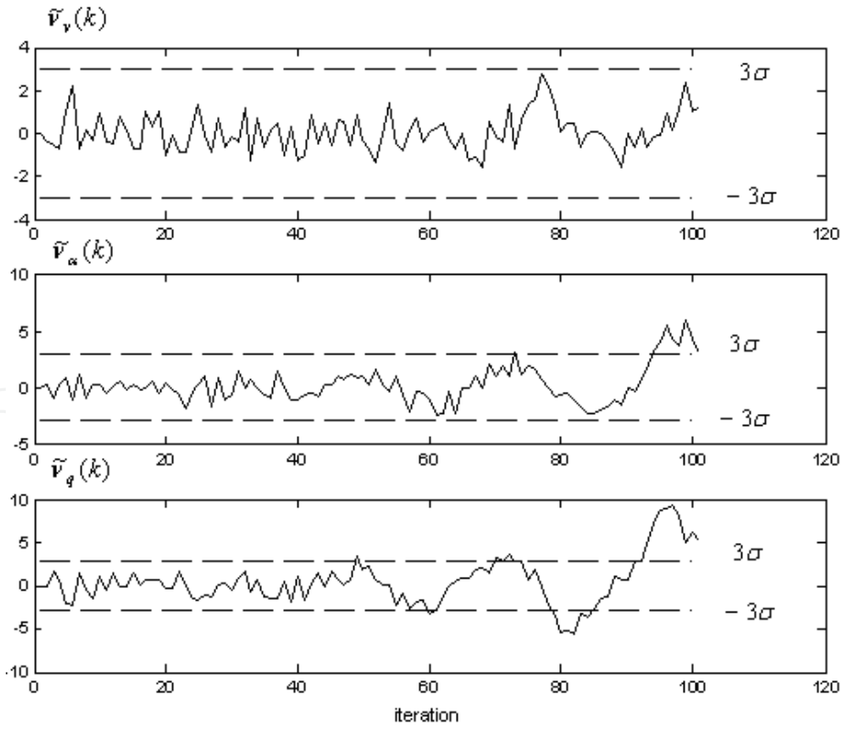

Fig. 14. Normalized Innovation Sequences $\tilde{\nu}_v(k), \tilde{\nu}_\alpha(k), \tilde{\nu}_q(k)$ in case of control surface failure

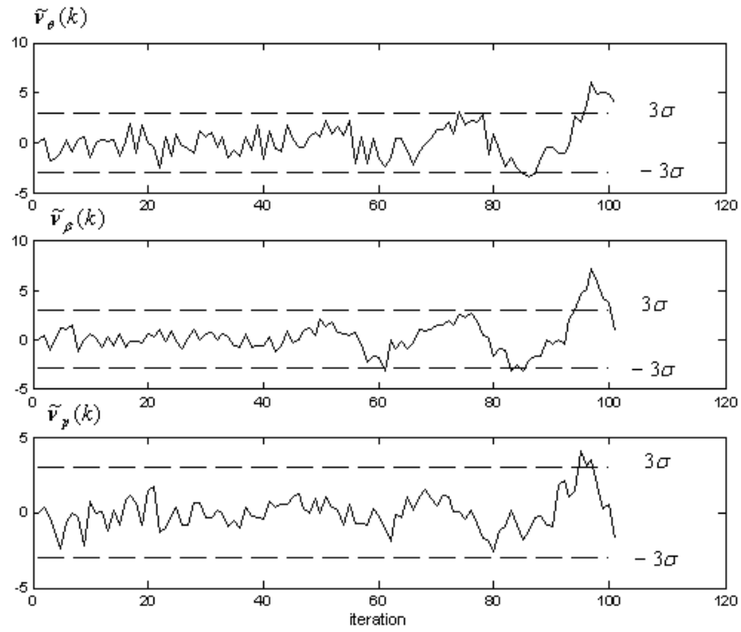

Fig. 15. Normalized Innovation Sequences $\tilde{\nu}_\theta(k)$, $\tilde{\nu}_\beta(k)$, $\tilde{\nu}_p(k)$ in case of control surface failure

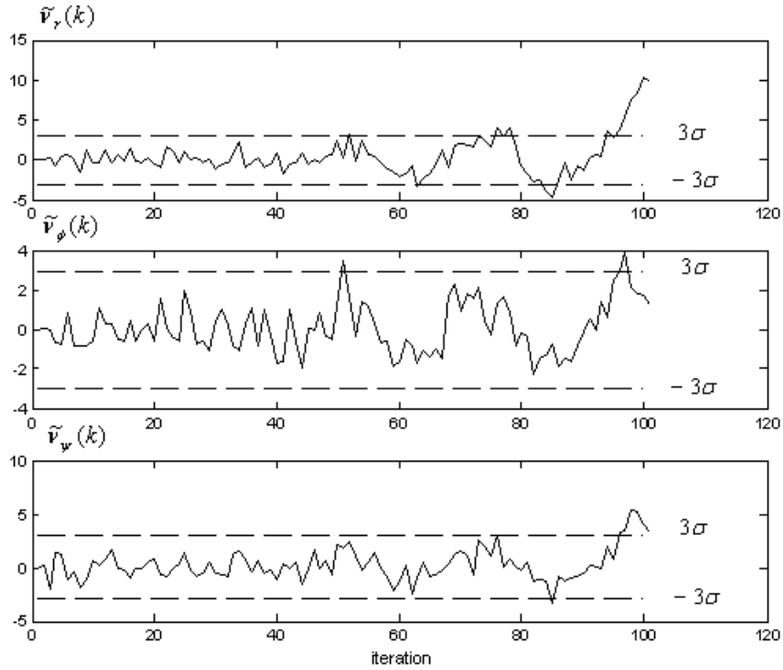

Fig. 16. Normalized Innovation Sequences $\tilde{\nu}_r(k)$, $\tilde{\nu}_\phi(k)$, $\tilde{\nu}_\psi(k)$ in case of control surface failure

The simulations show that both sensor and actuator/surface failures affect the spectral norm of the normalized innovation matrix. The simulation results justify the obtained

theoretical calculations and show the practical applicability of the proposed failure detection algorithm.
The introduction of the developed fault detection algorithms does not distort the estimation results of the filter and has no influence on their accuracy.
In real situations of exploiting an object, the proposed algorithm enables operative detection of faults such as: abnormal measurements, sudden shifts appearing in the measuring channel, faultiness of the measuring devices, changes in the statistical characteristics of the noises of an object or of measurements, reduction in the actuator/surface effectiveness, friction between moving parts of the control surfaces, partial loss of a control surface (break off of a part of control surface), malfunctions in the computer, and also a sharp change in the trajectory of a monitoring process, etc in order to subsequently correct estimators or to make timely decisions on the necessity and the character of the control actions with respect to the process of technical exploitation of the object.

4.5 Simulation Results of Adaptive EKF Insensitive to Sensor Failures

Simulation of the proposed adaptive EKF for the F-16 aircraft state estimation is performed. The measurements were processed using adaptive EKF (40) insensitive to sensor failures. To verify the hypothesis γ_0 and γ_1 in cases of the sensor and control surface/actuator failures, the spectral norm of the matrix constructed as (7) is used. Decisions as to reveal a failure in the system are made based on the rule (23). The results of simulations are shown in Figures 17–21.
Behavior of the spectral norm $\sigma_{\max}[A]$ in case of changes in the noise variance of the pitch rate gyroscope (sensor failure), when the adaptive EKF is used, is given in Figure 17. The noise variance of the pitch rate gyroscope has been changed corresponding to (43) at iteration 30.

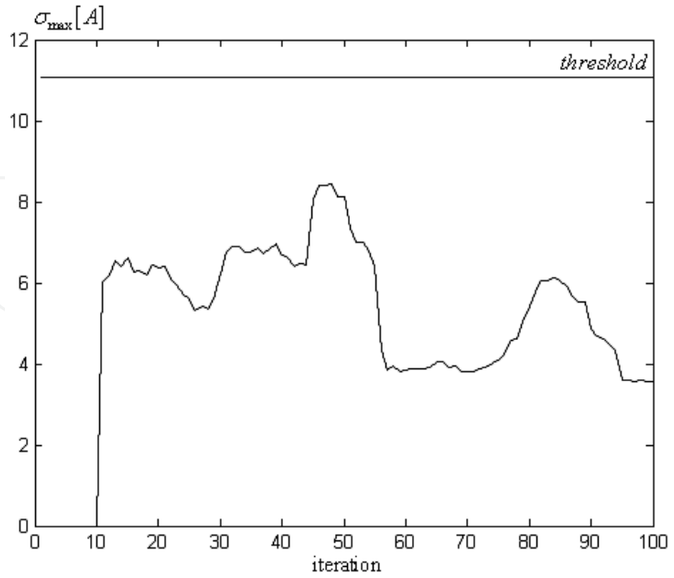

Fig. 17. Behavior of the spectral norm $\sigma_{\max}[A]$ in case of changes in the noise variance of the pitch rate gyroscope (adaptive EKF was used)

As seen in Figure 17, in spite of the sensor failure, in all iterations $\sigma_{max}[A]$ is lower than the threshold. Consequently, via the decision rule (23) γ_0 hypothesis is judged to be true. The normalized innovation sequence $\tilde{v}_q(k)$ in case of changes in the noise variance of the pitch rate gyroscope, when adaptive EKF is used, is shown in Figure 18. The results presented in the Figures 17 and 18 show that the adaptive EKF (40) is insensitive to sensor failures. Behavior of the weighting factor $S(k)$ of the adaptive filter is given in Figure 19. Behavior of the spectral norm $\sigma_{max}[A]$ in case of control surface failure, when adaptive EKF insensitive to sensor failures is used, is presented in Figure 20. The control derivatives corresponding to the first control surface (right horizontal stabilizer) has been changed corresponding to (44) at iteration 30. As seen in Figure 20, until the control surface failure occurs, $\sigma_{max}[A]$is lower than the threshold. When a fault occurs in the control surface, $\sigma_{max}[A]$ grows rapidly, and after 26 iterations it exceeds the threshold. Hence γ_1 hypothesis is judged to be true. The normalized innovation sequence $\tilde{v}_q(k)$ in case of control surface failure, when adaptive EKF is used, is given in Figure 21.

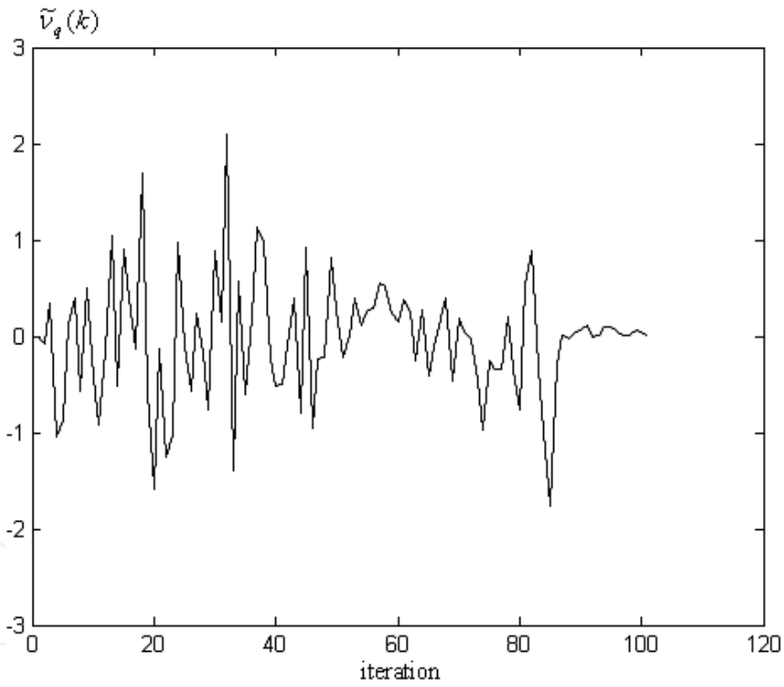

Fig. 18. Normalized Innovation Sequences $\tilde{v}_q(k)$ in case of changes in the noise variance of the pitch rate gyroscope (adaptive EKF was used)

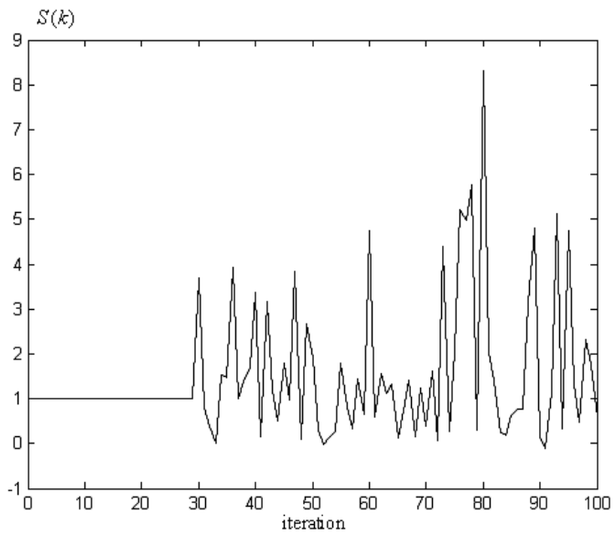

Fig. 19. Behavior of the weighting factor S(k)

The obtained simulation results show that the proposed adaptive EKF for the F-16 aircraft state estimation can isolate the detected sensor and actuator/surface failures. This filter is insensitive to sensor failures but sensitive to actuator/surface failures. When a regular EKF is used, the decision statistics changes regardless to the failure in the sensors or in the actuators/surfaces. On the other hand if the adaptive EKF insensitive to sensor failures is used, it is easy to distinguish the sensor and actuator failures.
The further fault isolation – finding in which component the fault has occurred (determining the location of the fault) - can be performed via the innovation approach based fault isolation methods described in (Hajiyev & Caliskan, 2003; Hajiyev & Caliskan, 2005; Hajiyev, 2009).

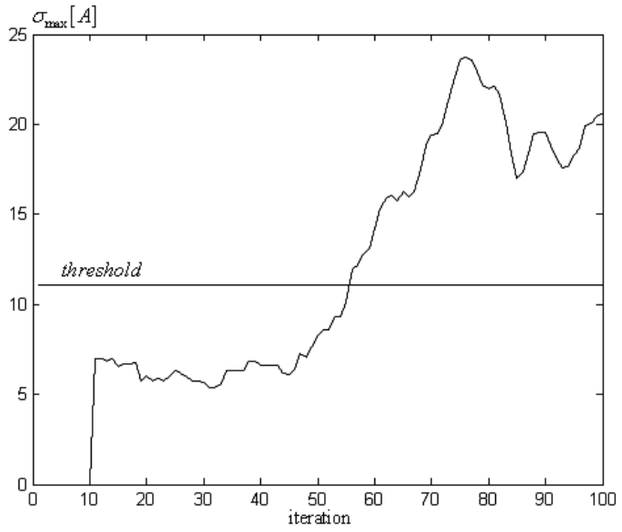

Fig. 20. Behavior of the spectral norm $\sigma_{max}[A]$ in case of the control surface failure (adaptive EKF was used)

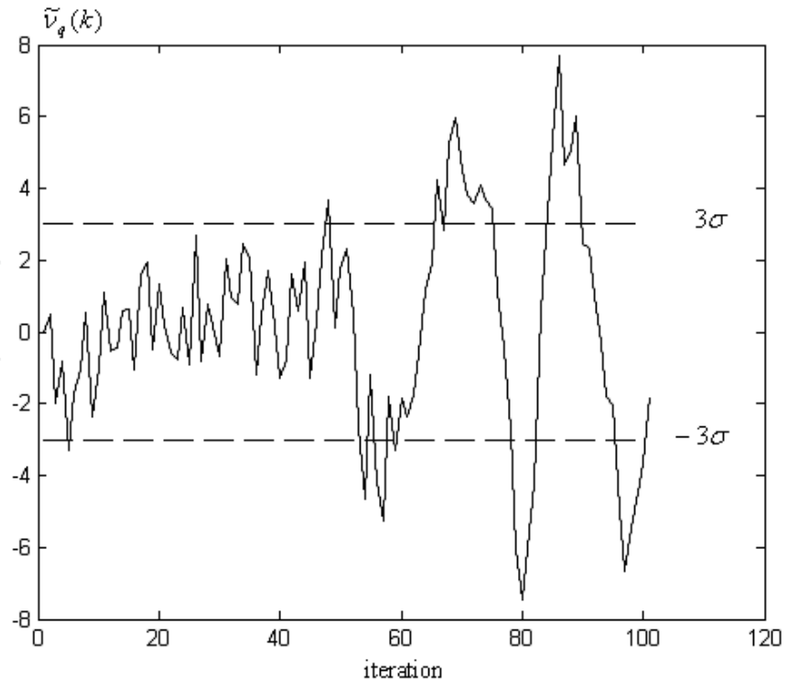

Fig. 21. Normalized Innovation Sequence $\tilde{v}_q(k)$ in case of the control surface failure (adaptive EKF was used)

4.6 About Choosing the Number of the Innovation Vectors (Samples)

Note that, in this case, the inertia (the delay) of the failure detection depends on the number of the innovation vectors (samples) m, that correspond to m different instants of time, from which the matrix of innovation A is composed and with an increase in this number, this characteristic worsens. On the other hand, a very small value of m leads to frequent false faults. Furthermore, the estimates of the eigenvalues of the matrix $A^T(k)A(k)$ and consequently, the singular values of the matrix $A(k)$ and the spectral norm of the matrix $A(k)$ will be biased for small sample sizes in general. Less unlikely larger number of the samples m causes to the biasness of the estimates. However, larger number of the samples reduces the ability of the algorithm to correctly trace high-frequency changes of the trajectory, e.g. turns (Mohamed & Schwarz, 1999). Therefore, the trade-off between the biasness and the frequent false faults on the one hand and the tractability of the estimates and bad inertia characteristic of the fault detection on the other hand should be taken into account according to the application at hand. In addition, the proper choice of the number of innovation vectors m, depends significantly on the motional dynamics. Since the number of samples m, is chosen empirically, there is no theoretically justified choice of it at present. Deriving the required correct detection and the false alarm characteristics involves mathematical simulation for a justified choice of the number of innovation vectors m. For this purpose simulations of the failure detection algorithm are performed for the different number of samples m. During simulations four kinds of scenario are considered:

1. In the simulations, m, n, and β are taken as $m = 6; n = 9; \beta = 0.95$, and the threshold value $\sqrt{\chi^2_{\beta,(nm-1)}}$ is found as 8.1. The noise variance of the pitch rate gyroscope is changed at iteration 30.
2. In the simulations, m, n, and β are taken as $m = 13; n = 9; \beta = 0.95$, and the threshold value $\sqrt{\chi^2_{\beta,(nm-1)}}$ is found as 11.91. The noise variance of the pitch rate gyroscope is changed at iteration 30.
3. In the simulations, m, n, and β are taken as $m = 30; n = 9; \beta = 0.95$, and the threshold value $\sqrt{\chi^2_{\beta,(nm-1)}}$ is found as 17.55. The noise variance of the pitch rate gyroscope is changed at iteration 60.

Decisions as to reveal a failure in the system are made based on the rule (23). The results of the simulations are shown in Figures 22–24. Graphs show the behavior of the statistic $\sigma_{max}[A]$ and its admissible bound in case of changes in the noise variance of the pitch rate gyroscope.

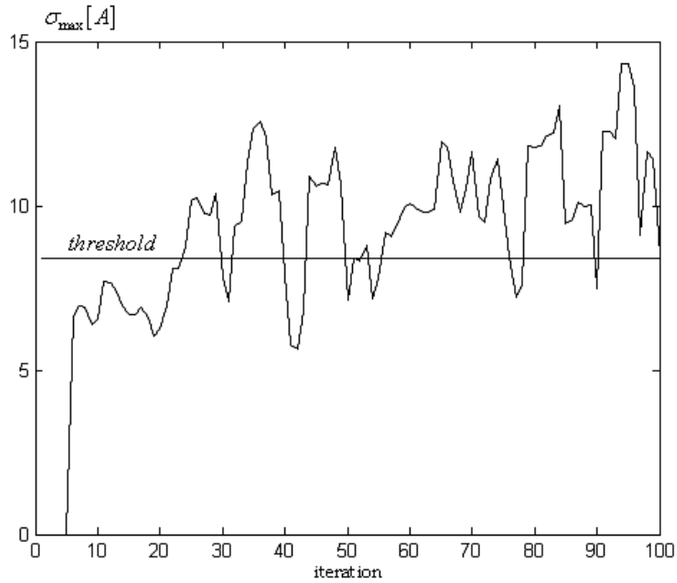

Fig. 22. Behavior of the spectral norm $\sigma_{max}[A]$ in case of changes in the noise variance of the pitch rate gyroscope at iteration 30 ($m = 6$)

As it is seen from Figure 22, in the first scenario ($m = 6$),the value of the statistic $\sigma_{max}[A]$ exceeds its admissible bound until the 30th step and via the decision rule (23) the false failure in the system is detected. When a failure occurs in the pitch rate gyroscope at the iteration 30, $\sigma_{max}[A]$ grows rapidly, and after 3 iteration (0.09 s after fault occurs) it exceeds the threshold. Hence γ_1 hypothesis is judged to be true. Figure 23 show that in the second scenario ($m = 13$), $\sigma_{max}[A]$ is lower than the threshold until the pitch rate gyroscope fault occurs. When a fault occurs in the pitch rate gyroscope at the 30th step,

$\sigma_{max}[A]$ grows abruptly and at the step $\tau = 37$ (0.21 s after fault occurs) it exceeds its admissible bound and the inequality (22) becomes not fulfilled. As a result, on the base of decision rule (23) failure in the system is detected. As seen from Figure 24, in the third scenario ($m = 30$), the statistic $\sigma_{max}[A]$ is lower than the threshold until the pitch rate gyroscope fault occurs. After the 60th step (after the fault occurs), the value of the statistic $\sigma_{max}[A]$ increases, and at the step $\tau = 84$ (0.72 s after fault occurs) it exceeds the threshold. Hence γ_1 hypothesis is judged to be true.

In the practical implementations the usage of the values between 10 and 20 are recommended for the number of samples m .

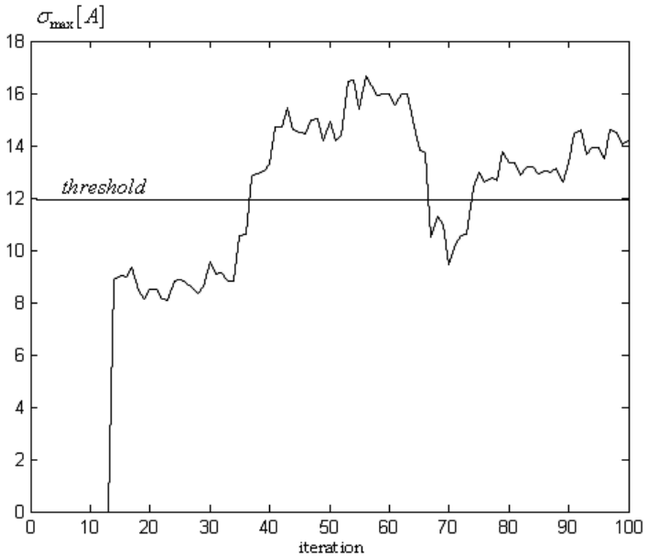

Fig. 23. Behavior of the spectral norm $\sigma_{max}[A]$ in case of changes in the noise variance of the pitch rate gyroscope at iteration 30 ($m = 13$)

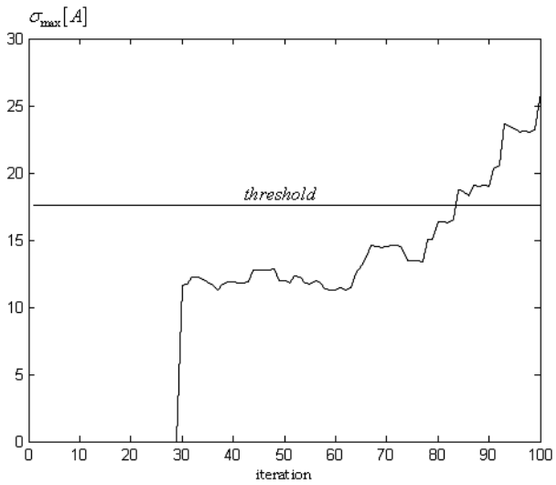

Fig. 24. Behaviour of the spectral norm $\sigma_{max}[A]$ in case of changes in noise variance in the pitch rate gyroscope at iteration 60 ($m = 30$)

5. Conclusions and Discussions

An approach to detect the aircraft sensor and actuator/surface failures based on the spectral norm of an innovation matrix is proposed. An upper confidence bound for the spectral norm of a random innovation matrix $A(k) \in R^{n \times m}$ that consists of normally distributed random variables with zero mathematical expectation is found. The outlined approach allows check of the mathematical expectation and the variance of the innovation sequence simultaneously online and does not require a priori information on the quantitative changes of its statistical characteristics in case of failure.
The suggested approach to the failure detection is used for the sensor and actuator/surface failure detection problem in the AFTI/F-16 aircraft flight control system. An extended Kalman filter has been developed for nonlinear flight dynamic estimation of an F-16 fighter. Failures in the sensors and actuators/surfaces affect the characteristics of the innovation sequence of the EKF. The failures that affect the mean and the variance of the innovation sequence have been considered. The following failures, that affect the characteristics of the innovation sequence of the EKF are examined:

a) Shift in the measurement noise of the pitch rate gyroscope (sensor failure);
b) Changes in the noise variance of the pitch rate gyroscope (sensor failure);
c) Shift in the control input, corresponding to the deflection of the right horizontal stabilizer (actuator motor failure);
d) Changes in the control derivatives corresponding to the right horizontal stabilizer (control surface failure).

The theoretical results are confirmed by the simulations carried out on a nonlinear dynamic model of the F-16 aircraft. The obtained simulation results have confirmed the practical possibility of the diagnostics of the flight control system using the introduced spectral norm of the innovation matrix. The introduction of the developed failure detection algorithm does not distort the estimation results of the filter and has no influence on their accuracy.
An adaptive EKF for the F-16 aircraft state estimation insensitive to sensor failures is designed and a decision approach to isolate the sensor and actuator/surface failure is proposed. When a regular EKF is used, the decision statistics changes regardless to the failure in the sensors or in the actuators/surfaces. On the other hand, if the adaptive EKF insensitive to sensor failures is used, it is easy to distinguish the sensor and actuator failures.
It is shown that the inertia of the fault detection depends on the number of samples m and with an increase in this number, this characteristic worsens. On the other hand, a very small value of m leads to frequent false faults. Some recommendations for the choice of the number of samples m in the practical implementations are given in this study.
The presented failure detection method has the following disadvantages: this method is of a statistical approach and a particular statistics must be accumulated, and the method has no ability to determine the value of the fault (fault identification).
The future work is to investigate the integrated sensor and actuator/surface failure detection, isolation and identification, and reconfigurable control problems together for the innovation approach based active fault–tolerant flight control system design.

6. References

Alessandri, A. (2003). Fault diagnosis for nonlinear systems using a bank of neural estimators. *Computers in Industry,* 52(3), pp. 271-289.

Anderson, T.W. (1984). *An Introduction to Multivariate Statistical Analysis*, 2nd edition. John- Wiley & Sons, Inc., New York, USA.

Basseville, M. & Benveniste, A. (Eds.) (1986). *Detection of Abrupt Changes in Signals and Dynamical Systems.* Springer-Verlag.

Benveniste, A., Basseville, M. & Moustakides, G.V. (1987). The asymptotic local approach to change detection and model validation. *IEEE Transactions on Automatic Control,* AC-32, pp. 583-592.

Bienvenu, G. & Kopp, L. (1983). Optimality of high resolution array processing using the eigensystem approach. *IEEE Transactions on Acoustics, Speech and Signal Processing*, 31**,** pp. 1235-1248.

Borairi, M. & Wang, H. (1998). Actuator and sensor fault diagnosis of non-linear dynamic systems via genetic neural networks and adaptive parameter estimation technique, In: *Proceedings of the IEEE Conference on Control Applications*. V.1, pp. 278-282.

Caliskan, F. & Hajiyev, Ch.(2003). Actuator Failure Detection and Reconfigurable Control for F-16 Aircraft Model. In: *Preprints of the 3rd IFAC Workshop "Automatic Systems for Building the Infrastructure in Developing Countries"(DECOM-TT 2003),* Istanbul, Turkey, pp. 231-236.

Chan, C.W., et al.(1999). On-line fault detection and isolation of nonlinear systems. In: *Proc. Amer. Control Conf. (ACC' 99),* San Diego, California, pp. 3980–3984.

Chen, J. & Patton, R.J. (1999). *Robust Model – Based Fault Diagnosis for Dynamic Systems.* Kluwer Academic Publishers, USA.

Edelman, A. (1991). The distribution and moments of the smallest eigenvalue of a random matrix of Wishart type. *Linear Algebra and its Applications*, 159**,** pp**.**55-80.

Everson, R. & Stephen, R. (2000). Inferring the eigenvalues of covariance matrices from limited noisy data. *IEEE Transactions on Signal Processing,* 48, pp. 2083-2091.

Grouffaud, J., Larzabal, P. & Clergeot, H. (1996). Some properties of ordered eigenvalues of a Wishart matrix: application in detection test and model order selection, *Proceedings of the IEEE International Conference on Acoustics, Speech, and Signal Processing, ICASSP*, Atlanta, GA, USA, 5, pp. 2463-2466.

Gadzhiev, Ch. M. (1992). Dynamic systems diagnosis based on Kalman filter updating sequences. *Automation and Remote Control*, 1, pp. 147-150.

Gadzhiyev, Ch. M. (1993). Checking multivariate model fit from the generalized Wishart-statistic variance. *Measurement Techniques*, 36(12), pp. 1316-1319.

Gadzhiev, Ch. M. (1996). *The Information Provision of Offshore Platform Supervision and Control* (in Russian), Elm, Baku.

Grishin, Yu. P. & Kazarinov, Yu. M. (1985). *Fault-Tolerant Dynamic Systems* (in Russian), Radio i Svyaz, Moscow.

Hajiyev, Ch. & Caliskan, F. (2003). *Fault Diagnosis and Reconfiguration in Flight Control Systems.* Kluwer Academic Publishers, Boston.

Hajiyev, Ch. & Caliskan, F. (2005). Sensor and control surface/actuator failure detection and isolation applied to F-16 flight dynamics. *Aircraft Engineering and Aerospace Technology: An International Journal*, 7, pp. 152-160.

Hajiyev, Ch. (2006). Adaptive filtration algorithm with the filter gain correction applied to integrated INS/Radar altimeter, *Proceedings of the 5th International Conference on Advanced Engineering Design,* Prague, Czech Republic.

Hajiyev, Ch. (2007). Sensor and Control Surface/Actuator Failure Detection Based on the Spectral Norm of an Innovation Matrix. In: *Preprints of the 17th IFAC Symposium on Automatic Control in Aerospace*, Toulouse, France, Paper No.22.

Hajiyev, Ch. (2009). Innovation approach based sensor FDI in LEO satellite attitude determination and control system. In the book: *Kalman Filter: Recent Advances and Applications,* I-Tech Education and Publishing KG, Vienna, Austria, pp. 347-374.

Horn, R. & Jonson, Ch. (1986). *Matrix Analysis*, Cambridge University Press, Cambridge, UK.

Kendall, M.G. & Stuart, A. (1969). *The Advanced Theory of Statistics*. Griffin, London, UK.

Krinetsky, Ye.I., *et al.*, (1979). *Flight Testing of Rocket and Space Apparatus* (in Russian), Mashinostroyeniye, Moscow.

Larson, E.C., et al. (2002). Model-based sensor and actuator fault detection and isolation. In: *Proceedings of the American Control Conference*, V. 5, pp. 4215-4219.

Lee, J.H. & Lyou, J. (2002). Fault diagnosis and fault tolerant control of linear stochastic systems with unknown inputs. *Systems Science*, 27(3), pp. 59-76.

Li, Z. & Jaimoukha, I.M. (2009). Observer-based fault detection and isolation filter design for linear time-invariant systems, *International Journal of Control*, 82, pp. 171-182.

Lyshevski, S.E. (1997). State-space identification of nonlinear flight dynamics. In: *Proceedings of the Conference on Control Applications,* Hartford, Connecticut, pp. 496-498.

Malik, R.K. (2003). The pseude-Wishart distribution and its application to MIMO systems. *IEEE Transactions on Information Theory,* 49, pp. 2761-2769.

Maybeck, P.S. (1999). Multiple model adaptive algorithms for detecting and compensating sensor and actuator/surface failures in aircraft flight control systems. *International Journal of Robust and Nonlinear Control*, 9(14), pp.1051-1070.

Mehra, R.K. & Peschon, J. (1971). An innovations approach to fault detection and diagnosis in dynamic systems. *Automatica,* 7, pp. 637-640.

Mohamed, A.H. & Schwarz, K.P. (1999). Adaptive Kalman filtering for INS/GPS. *Journal of Geodezy,* 73, pp. 193-203.

Napolitano, M.R., Chen, Ch. & Naylo, S.(1993). Aircraft failure detection and identification using neural networks. *Journal of Guidance, Control, and Dynamics*, 16(6), pp. 999-1009.

Napolitano, M.R., et al. (1996). Online learning neural architectures and cross-correlation analysis for actuator failure detection and identification. *International Journal of Control*, 63(3), pp. 433-455.

Perhinschi, M.G., et al. (2002). On-line parameter estimation issues for the NASA IFCS F-15 fault tolerant systems. In: *Proceedings of the American Control Conference*, V.1, pp. 191-196.

Rago, C., et al. (1998). Failure Detection and Identification and Fault Tolerant Control using the IMM-KF with applications to the Eagle-Eye UAV. *Proceedings of the IEEE Conference on Decision and Control,* V 4, pp. 4208-4213.

Rao, S.R. (1965). *Linear Statistical Inference and Its Applications*, New York, John Wiley & Sons, Inc.

Raza, H., Ioannou, P. & Youssef, H.M. (1994). Surface failure detection for an F/A-18 aircraft using neural networks and fuzzy logic. In: *Proceedings of the IEEE International Conference on Neural Networks*, V 5, pp. 3363-3368.

Sage, A.P. & Melsa, J.L. (1971). *Estimation Theory with Applications in Communication and Control.* McGraw-Hill, New York.

Tykierko, M. (2008). Using invariants to change detection in dynamical system with chaos. *Physica D: Nonlinear Phenomena*, 237, pp. 6-13.

Vaswani, N. (2004). Change detection in partially observed nonlinear dynamic systems with unknown change parameters. *Proceedings of the American Control Conference (ACC'2004),* pp. 5387-5393.

Wax, M. & Kailath, T. (1985). Detection of signals by information theoretic criteria. *IEEE Transactions on Acoustics, Speech and Signal Processing*, 33, pp. 387-392.

Willsky, A.S.(1976). A survey of design methods for failure detection in dynamic systems. *Automatica,* 12(6), pp. 601-611.

Wu, H.T., Yang, J.F. & Chen, F.K. (1995). Source number estimators using transformed Gerschgorin Radii. *IEEE Transactions on Signal Processing*, 43, pp. 1325-1333.

Zanella, A., Chiani, M. & Win, M.Z. (2008). A general framework for the distribution of the eigenvalues of Wishart matrices, *Proceedings of the ICC-2008 conference*, pp. 1271-1276.

Zhang, Y. & Li, X.R. (1997). Detection and diagnosis of sensor and actuator failures using Interacting Multiple-Model estimator, *Proceedings of the IEEE Conference on Decision and Control*, V.5, pp. 4475-4480.

Fault Detection

Edited by Wei Zhang

ISBN 978-953-307-037-7
Hard cover, 504 pages
Publisher InTech
Published online 01, March, 2010
Published in print edition March, 2010

In this book, a number of innovative fault diagnosis algorithms in recently years are introduced. These methods can detect failures of various types of system effectively, and with a relatively high significance.

INTECH
open science | open minds

InTech Europe
University Campus STeP Ri
Slavka Krautzeka 83/A
51000 Rijeka, Croatia
Phone: +385 (51) 770 447
Fax: +385 (51) 686 166
www.intechopen.com

InTech China
Unit 405, Office Block, Hotel Equatorial Shanghai
No.65, Yan An Road (West), Shanghai, 200040, China
中国上海市延安西路65号上海国际贵都大饭店办公楼405单元
Phone: +86-21-62489820
Fax: +86-21-62489821

IntechOpen